

Molecular Docking, ADMET Study, Synthesis, Anti-inflammatory, and Antimicrobial Screening of New NSAIDs Conjugated with Gabapentin

Noor W. Saleh Rabee¹   and Tagreed N-A Omar^{*2}  

¹ Ministry of Health, Najaf, Iraq

² Department of Pharmaceutical Chemistry, College of Pharmacy, University of Baghdad, Baghdad, Iraq

*Corresponding author

Received 2/6/2024, Accepted 8/9/2024, Published 15/2/2025



This work is licensed under a Creative Commons Attribution 4.0 International License.

Abstract

Non-Steroidal anti-inflammatory drugs NSAIDs are used to treat a wide range of painful conditions. They are known for their properties as analgesic, antipyretic, and anti-inflammatory.

Focusing on the synthesis of new NSAIDs derivatives (IIa-IVd) through introducing ester group at its COOH group with Gabapentin through a acetyl linker. The process involved the formation of Schiff base; intermediates (Ia-b) from gabapentin and *p*-substituted benzaldehyde. (Etodolac, Ketorolac, and Tolmetin) undergo esterification by chloroacetyl chloride to give the corresponding esters (II-IV), finally Ia-d reacted with (II-IV) to yield the final derivatives (IIa – IVd) which were confirmed for their purity and structure by melting point, (ATR-FTIR) and ¹HNMR. In vitro and in vivo the anti-inflammatory, antibacterial activities and ADME were evaluated using Ligand Designer from Glide (Schrödinger-2023-Maestro workspace).

Due to their hydrogen bonding interaction with key amino acids in COX1 enzyme, (IIIa, IIIc & IIIe) have the highest docking score, and COX2 enzyme (IIIa and IIa). Regarding to antibacterial activity, all of them are significant except only IVb. The compounds (IIIa, IIIc & IIIe) have the highest docking scores (-8.22, -7.07 & -6.155) respectively. ADME analysis revealed the highest results as TPSA: (IIIa, IVa & IIc); -(IIa, IIb, IIc & IId) as hydrogen bond donor; -as hydrogen bond acceptor (IIa, IIIa & IVa); -logP o/w: (IIIc, IIb & IIc); logS -: (IIb, IIIc & IIc); and finally-Rotatable bond: (IIc, IVa & IVc); the others compounds' *insilico* ADMET screening findings fall within the advised ranges.

In vivo, the anti-inflammatory; IIa-IVd showed good activity from 2-3 h. As antimicrobial activity, the high activity given by: *S. aureus*: (IVb, IVc & IIa); *S. pneumoniae*: (IIIc, IVb & IVd); *B. subtilis*: (IVb, IVc & IIIc); *E. coli*: (IVb, IVc & IIa); *P. aeruginosa*: (IVb & IVc); *K. pneumoniae* (IVb, IIIc & IIa); give high activity; the others ranging (moderate- inactive). Antifungal activity against *Candida albicans*, when compared with the drug fluconazole, (IVb); the other final compounds were (moderate-inactive). The compounds were successfully synthesized, and the results of the study of anti-inflammatory and antibacterial effectiveness indicate that the final compounds contain drug-like features.

Keywords: ADMET, Gabapentin, Molecular Docking, NSAIDs derivatives, Etodolac, Ketorolac, Tolmetin

Introduction

The class of nonsteroid anti-inflammatory drugs (NSAIDs) like Etodolac (1), Ketorolac (2) and tolmetin (3) that are represented in Figure 1 constitute a group of heterogeneous molecules that commonly used medications worldwide ⁽¹⁾ This drug class possess many pharmacological activities such as analgesic, anti-pyretic, and edema-reducing effect, so they are used for the long and short term management of various conditions, include osteoarthritis, rheumatoid arthritis, and musculoskeletal pain ⁽²⁾.

Some research suggests that etodolac and tolmetin may have a lower risk of adverse cardiovascular events, such as heart attack or stroke, compared to NSAIDs like diclofenac or ibuprofen ⁽³⁾. (NSAIDs) have shown significant potential in

both the prevention and treatment of various cancers, as evidenced by extensive research. Chronic inflammation is a well-established factor in carcinogenesis, and NSAIDs, by inhibiting the Cyclooxygenase (COX) pathway, reduce the production of pro-inflammatory prostaglandins, thereby mitigating inflammation-induced cancer progression ^(4,5).

However, the relationship between the oral intake of non-steroidal anti-inflammatory drugs (NSAIDs) and gastrointestinal (GI) side effects is well-documented and multifaceted, and range from dyspepsia, heartburn, and abdominal discomfort to more serious events such as peptic ulcer with the life-threatening complications of bleeding and perforation ⁽⁶⁾.

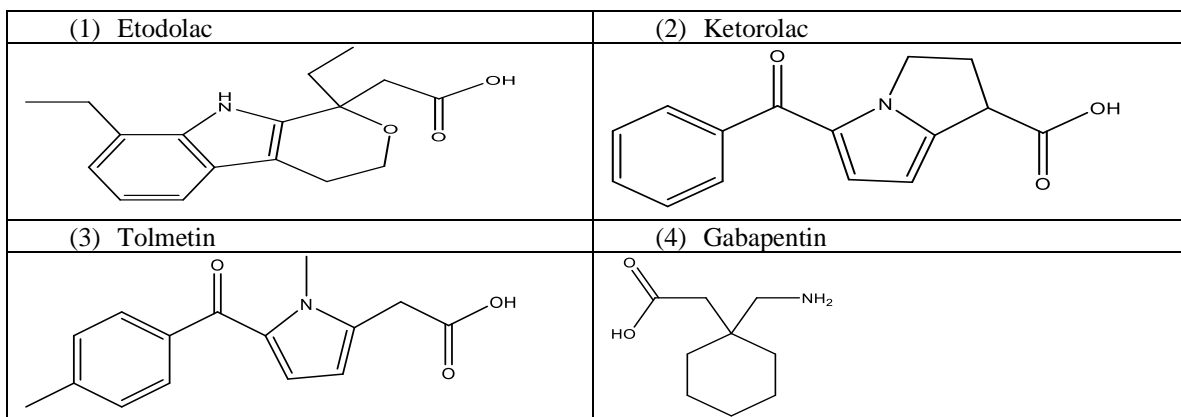


Figure 1. Chemical structures of some NSAIDs and gabapentin .

One of the most effective strategies to prevent the gastric irritation commonly associated with non-steroidal anti-inflammatory drugs (NSAIDs) is the derivatization of their carboxylic acid group. These modifications not only retain the anti-inflammatory efficacy of the parent NSAIDs but also offer opportunities for optimizing drug efficacy and safety profiles through structural alterations, highlighting the importance of strategic derivatization in drug development⁽⁷⁻⁹⁾. This approach involves the design and synthesis of products, which are bio reversible derivatives that undergo enzymatic or chemical transformation *in vivo* to release the active drug. By masking the carboxylic acid group, products can significantly reduce gastrointestinal side effects⁽¹⁰⁾. Esterification is a common method used to create these products. This strategy is particularly effective because ester products can mask the free carboxylic acid group, thereby reducing gastrointestinal side effects and enhancing the drug's overall bioavailability and patient compliance⁽¹¹⁾.

Research indicates that ester products, such as those synthesized from naproxen, can show varied efficacy based on their hydrolysis rates.⁽¹²⁾ This resistance to hydrolysis is a common challenge with ester products, as seen with other NSAIDs like aspirin and ibuprofen. Ester derivative products have been found cleavable enzymatically to release its bioactive forms and, the activity of these enzymes can vary significantly among individuals due to genetic differences, and environmental factors, leading to substantial variability in drug bioavailability^(13,14). To address the limitations above, anhydride derivatives of carboxylic acid-bearing drugs present a promising alternative to traditional ester products. Unlike ester bonds, which are commonly used in products to mask free carboxylic acid groups and reduce gastrointestinal side effects, anhydride bonds offer a more predictable hydrolysis and decomposition pattern. This predictability is due to the inherent chemical properties of anhydrides, which readily undergo hydrolysis, making them less sensitive to enzymolysis

compared to esters or amides⁽¹⁵⁾. One of the significant challenges in the development of ester and anhydride products is ensuring their stability against hydrolysis by saliva and gastrointestinal (GIT) fluids, allowing them to reach the target tissue effectively⁽¹⁶⁾.

To prevent anhydride and ester products from hydrolyzing before reaching their target tissue, several strategies can be employed, focusing on enhancing the stability of these compounds against hydrolytic degradation. One effective approach is the use of moisture barrier film coatings, additionally, the synthesis of anhydride products can be tailored to temporarily hydrophobized the drug, making it less accessible to aqueous media until the anhydride residue is hydrolyzed. This approach not only shields the carboxylic acid group from irritative effects but also prolongs the drug's action by controlling its release and activation in the body⁽¹⁷⁾. One of the most advantages of anhydride drugs is to achieve sustained release over extended periods through the strategic design of their polymer matrices and the inherent properties of anhydride bonds. The high hydrolytic reactivity of anhydride linkages is a key factor, as it allows for controlled degradation rates, which can be finely tuned by altering the chemical structure of the polymer backbone⁽¹⁸⁾.

Schiff bases, including imines, exhibit significant antibacterial and antifungal properties due to their unique chemical structure, which includes the presence of nitrogen heteroatom. This heteroatom play a crucial role in the biological activity of Schiff bases by facilitating interactions with microbial cell components, thereby disrupting their normal functions⁽¹⁹⁾, the structural diversity and the presence of functional groups in Schiff bases contribute to their potent antibacterial and antifungal activities, making them promising candidates for the development of new antimicrobial agents⁽²⁰⁾.

Gabapentin, an anticonvulsant structurally similar to gamma-aminobutyric acid (GABA), has been explored for its potential as a short-term adjunct in various pain management strategies. Its

primary use is in treating neuropathic pain and seizures, but its application extends to other conditions such as alcohol withdrawal symptoms, pruritus, hot flashes during menopause, and anxiety disorders. It is also effective in managing acute post-operative pain, providing a valuable option for short-term pain relief⁽²¹⁾. The combination of the gabapentin with NSAIDs medications has been shown to be effective in various pain models. Mutual prodrug, where the carrier used is another biologically active drug instead of some inert molecule. A mutual prodrug consists of two pharmacologically active agents coupled together so that each act as a pro-moities for the other agent and vice versa. The carrier may also be a drug that might help to target the parent drug to a specific site or organ or cells or may improve site specificity of a drug. The carrier drug may be used to overcome some side effects of the parents' drugs as well. Thus, the mutual prodrug approach is of a great interest, because combination therapy of two separate drugs is used to treat many diseases where the actives should be administered in separate dosage forms⁽²²⁻²⁴⁾.

In the current work, we are focusing on the synthesis of mutual prodrugs were synthesized by conjugating different types of NSAIDs with gabapentin using chloroacetyl chloride spacers in order to ameliorate the NSAID's gastric irritation by esterification of the free carboxyl group, and produce a synergistic analgesic effect from use two analgesic drugs, so coupling with different types of NSAIDs will have an additional benefit for treatment of neuropathic pain with enhanced patient compliance from use of a single chemical entity.

Materials and Methods

Chemicals and Instruments

Gabapentin, Etodolac, ketorolac and tolmetin were supplied from (Macklin, China). All solvents and reagents that used received from the chemicals store of college. Melting points were determined by digital melting point apparatus (Stuart SMP30). The purity of the products and the monitoring of the reactions check was done by thin layer chromatography (TLC). ¹H-NMR spectra were obtained on BRUKER model Ultra shield 500 MHz spectrophotometer, using Dimethyl sulfoxide (DMSO) as a solvent.

By using FTIR Spectrometer (Shimadzu, Japan), FTIR spectra were recorded, at college of Pharmacy-University of Baghdad.

In Silico Design

In silico experiment

The docking method began by obtaining the crystal structure of the COX-1 protein (PDB code: 3N8Z), COX-2 protein (PDB code: 4m11) Diclofenac as a reference, and the crystal structure of the penicillin binding protein 3 of Mycobacterium tuberculosis (6KGV) from the Protein Data Bank. Subsequently, thorough protein preparation was a

place within the Schrödinger-2023-Maestro workspace. In this step, water molecules that were not involved in the binding site were removed. Afterwards, the hydrogen bonds were optimized to minimize any possible overlap problems, thereby assuring a precise depiction of the binding environment. The optimization approach was essential for enhancing the protein's structural integrity in anticipation of the forthcoming docking procedure. Concurrently with the production of proteins, meticulous processes for preparing ligands were carried out. The ligands were carefully designed to mimic their possible states within a pH range of 7 ± 2 . Using the OPLS4 force field, the ligands were subjected to desalting in order to eliminate unnecessary ions and improve the accuracy of their molecular structures⁽²⁵⁾. In addition, all possible tautomers were created to cover the wide range of chemical variations that the ligands could display within the normal pH range of the body. The extensive ligand preparation step established the basis for a comprehensive investigation of ligand-protein interactions during the docking procedure. After preparing both the protein and ligand appropriately, the subsequent stage consisted of creating a receptor grid using the reference ligand, FLP. The reference ligand was positioned at the center of the binding pocket, acting as a central point for generating the receptor grid. A cubic box measuring 25 Å in dimensions for COX-1, COX-2 and 30 Å for PBP3 were created around the reference ligands to define the spatial limits for the following docking simulations. The careful creation of a precise grid allowed the docking algorithm to thoroughly examine possible binding positions within the limited space of the binding pocket. Lastly, standard precision docking with flexible sampling was carried out using the Glide docking algorithm. This approach made it easier to investigate different ligand orientations and conformations inside the receptor binding region, enabling a thorough investigation of possible binding interactions. Flexible sampling was used to guarantee a robust docking approach that captured the complex interactions between the ligands and the COX-1 and COX-2 proteins. All things considered, this methodical approach—which included exact preparation of the protein and ligand as well as grid generation and docking simulations—constituted a thorough means of clarifying the interactions between the protein and ligand inside the COX-1 and COX-2 binding pocket^(26,27).

ADMET studies

To test the drug resemblance of proposed compounds, ligand-based ADMET prediction is a crucial step, utilizing software like Swiss ADME to identify the most similar drug molecules. This process involves evaluating various molecular properties, including the number of hydrogen bond acceptors and donors, as outlined in Lipinski's rule of five, which is essential for predicting oral bioavail-

ability. Swiss ADME is a pivotal tool in the drug design methodology, suite of predictive models to evaluating the physicochemical properties, pharmacokinetics, drug-likeness, and medicinal chemistry friendliness of small molecules⁽²⁵⁾.

Chemical synthesis

Synthesis of gabapentin- *p*-substituted benzaldehydes as Schiff base (Ia-b)⁽²⁶⁻²⁸⁾

Solution of gabapentin (1.712g , 10 mmol) and absolute methanol (99%) (40ml) in (100ml) round bottom flask were mixed with stirring ,then 10 mmol of *p*-substituted benzaldehyde (a: NO₂ 1.51 g, b : Br 1.85 g) and 1-3 drops of glacial acetic acid in absolute methanol (3ml) was added .The reaction mixture was reflux for (5 h) at temperature 60 - 80 °C. After the completion of the reaction, absolute methanol was removed by rotary evaporator; yellow residue was collected and recrystallized from absolute methanol (99%) to give yellow crystals of Schiff base Ia-b.

Synthesis of NSAIDs -chloroacetyl chloride derivatives comps. (II - VI)^(27,29)

An appropriate amount of each NSAIDs 10 mmole(2.87 gm (Etodolac) – 2.55 gm (Ketorolac) - 2.57 gm (Tolmetin)) was mixed respectively with trimethylamine (0.01mole,1.4ml), 25ml of dichloromethane was placed above the mixture in a round bottom flask and then the mixture was cooled to -10°C, using an ice bath . A mixture of chloroacetylchloride (0.01mole/0.8ml) in chloroform 25ml was prepared and was added drop-wise to the mixture over a period of 1hr, with continuous stirring, the temperature of reaction mixture was kept at -10°C during the addition; the resultant mixture was stirred over night at -10°C. Then washing using separatory funnel with three different solutions as follows; 5% NaOH (3×50 ml), 5% HCl (3×50 ml), Brine solution (2×25ml). The intermediate of the NSAIDs -chloroacetylchloride was collected by evaporating the solvent using a hot air stream. Then recrystallization was done with petroleum ether (60-80) °C and ethyl acetate (25:1)

Synthesis of mutual prodrugs target compounds (II - VI)⁽³⁰⁾

The following mixtures were prepared: Compound I 10 mmole (3.04 gm (a) , 3.38 gm (b)) , Compound II Chloro - acetyl derivatives 10 mmole (3.63 gm (a) – 3.31gm (b) – 3.33gm (c)) , TEA (10 mmole/1.4ml) , sodium iodide (10mmole/1.5gm) in DMF 25ml was stirred overnight at 25 °C. Then after, poured down into ice slush, stirred, and extracted using Chloroform solution (25 ml, used four times).

The resultant organic layer was washed over with 50 ml of 2% Na₂S₂O₃ (3x50 ml), 5% NaOH (3×50 ml), 5% HCl (3×50 ml), Brine solution (2×25ml). The organic layer dried over anhydrous sodium sulphate and was filtered using under pressure circumstances to remove the solvent to obtain the

Gabapentin – NSAIDs mutual prodrugs (II-VI)a,b. The derivatives then re – crystallized from Petroleum Ether (60-80) and Ethyl – Acetate (25:1).

Preliminary Pharmacological Study

Anti-Inflammatory assessment Study⁽³¹⁾

The anti-inflammatory properties of the synthesized compounds were assessed by evaluating the decrease in paw thickness of rats with egg-white-induced paw edema. This method involves measuring the reduction in paw edema thickness in vivo. The experiment protocol for evaluating the acute anti-inflammatory activity of synthesized derivatives (II-IV)a-d was conducted using the egg-white induced paw edema method in albino rats (AR), which aligns with established methodologies for assessing anti-inflammatory efficacy.

Methods^(32,33)

Sixty white albino rats weighing (160-200g) were attained from / Baghdad University animal house and kept in the Iraqi Center for cancer and Medical Genetics Research, they housed under standard conditions with marketable chaw as food and ad libitum water. Inflammation was measured at the start and throughout the short time course by subcutaneous injection of egg whites into the rat paw under standard acclimation conditions.

These rats were aimlessly sorted into 10 groups each group conforming of six rats: Group A: Six rats injected intra-peritoneally (IP) with propylene glycol considered as control. Group B: Six rats injected with reference drug (Diclofenac sodium 3mg/Kg dissolved in propylene glycol.The (C-H) Groups: Six rats from each group were injected with prepared compounds dissolved in propylene glycol in the doses shown in the table. 1 A 0.05ml subcutaneous injection of undiluted egg-white material into the plantar side of the left hand paw for the rats' hind paws may cause substantial skin discomfort, due to dominant inflammation. Thirty minutes after the administration of the desired compounds or the vehicle, the paw width was measured using a Vernier caliper at intervals of (0, 30, 60, 120, 180, 240, and 300) minutes, respectively, after drug administration.

Dose Calculation

The doses of these target compounds were calculated according to the following equation⁽³⁴⁾:

$$\frac{\text{Dose of reference compound}}{\text{M.wt of reference compound}} =$$

$$\frac{\text{Dose of tested compound}}{\text{M.wt of tested compound}}$$

$$\text{M.wt of tested compound}$$

Diclofenac sodium is given at a dose of 3 mg/kg, were the intended compounds are calculated in equation as shown in the Table (1):

Table 1. The molecular weights and doses for Diclofenac and the intended Compounds

Compounds	M.Wt	Rat dose(mg/kg)
Diclofenac sodium	318.1	3
IIa	631.726	5.957
IIb	665.625	6.277
IIIa	599.640	5.655
IIIb	633.539	5.974
IVa	601.656	5.674
IVb	635.555	5.993

Antimicrobial activity ⁽³⁵⁾

The minimum inhibitory concentration (MIC), alongside the agar diffusion method were used to assess the antimicrobial activity of the final compound (IIa – IVb) against various microorganisms, including Gram-positive bacteria (*Staphylococcus aureus* , *Streptococcus pneumoniae* , and *Bacillus subtilis*), Gram-negative bacteria (*Escherichia coli* , *Pseudomonas aeruginosa* , and *Klebsiella pneumoniae*), and fungi was *Candida albicans*.

Standard Mcfarland solution (tube No. 0.5)

Standard Mcfarland solution No. 0.5 was prepared according to Baron *et al*, 1994 as follows :

- 1- Solution (A) : dissolving 1.175 gm of barium chloride in 90ml of D.W then completed to 100 ml .
- 2- Solution (B) : adding 1 ml of conc. H₂SO₄ in 90ml of D.W and then completed to 100 ml .

The two solutions were mixed by adding 0.5 ml of solution (A) to 99.5ml of solution (B).The prepared solution was used to compare the turbidity of bacterial suspension in order to obtain an approximate cell density of 1.5×10⁸ CFU/ml.

Minimum inhibitory concentration reagent

The resazurin (Alamar Blue) solution was prepared by dissolving 0.015 g of resazurin in 100 ml sterile distilled water, a vortex mixer was used until well dissolved and stored at 4°C for a maximum of one week after preparation ⁽³⁶⁾.

Preparation of the Culture Media

All of the culture media were prepared according to the manufacturing company instructions. All these media were autoclaved at 121°C for 15 minutes at 15 pound per square inch (Psi). There were incubated for 24h at 37°C for the sterility test and store at 4°C until use ⁽³⁷⁾.

MIC test

At concentrations ranging from 10- 1000 mcg/ml, several diluted solutions were created from a stock solution (10 mg/ml) of each derivative. These solutions were prepared on a microtiter plate. The use of Mueller-Hinton broth as the diluent and the inoculation with a bacterial suspension equivalent to McFarland standard no. 0.5 (1.5×10⁸ CFU/ml) is consistent with established protocols for MIC determination ⁽³⁸⁾. The addition of resazurin dye, a redox indicator that changes

color in response to bacterial metabolic activity, allows for the visual determination of bacterial growth inhibition. The incubation period of 18 to 20 hours at 37°C is standard for such assays, ensuring sufficient time for bacterial growth and interaction with the antimicrobial agents. Following the incubation period, 20 µl of resazurin dye was introduced into each well. The subsequent 2-hour incubation with resazurin dye to observe color changes from blue to pink provides a clear visual endpoint for determining sub-MIC concentrations, which are the lowest concentrations at which bacterial growth is inhibited but not completely eradicated⁽⁴⁶⁾.

Therefore, conducting an MIC test prior to the well diffusion method provides a robust foundation for understanding the effective concentration of antibiotics, facilitating more accurate and reliable antimicrobial susceptibility testing and aid in the development of new antimicrobial agents^(39,40).

Sensitivity Assay⁽⁴¹⁾

The well diffusion assay used a bacterial culture of 1.5×10⁸ CFU/ml from the McFarland turbidity standard (Number 0.5). The procedure involved applying the substance to the surface of MHA plates using a swab and allowing the excess fluids to dry in a sterile hood. Four wells were created in each agar plate containing the microorganisms under examination, and 80µL of the test chemical was added to each well. The plates were then placed in an incubator at 30 °C for 72 hours for fungal species and at 37 °C for 24 hours for bacterial species. The zone of inhibition (ZI) width around each well was measured in millimeters to assess the antimicrobial activity.

Statistical analysis

All the experiments were performed and reported triplicate. The average mean values were reported along with standard deviation values. The t-test was conducted after verifying the normality and homogeneity of the data to assess its significance and compare the means (* <0.05;** <0.01; *** <0.001). The software used for statistical analysis is (R Studio 4.5 was used for the correlations and the figures by OriginLab 2021Software).s

Results and Discussion

In Silico Design

Docking study

The docking results for the final derivatives (IIa-IVd), including: the binding mode, docked pose, and binding free energy, were examined to assess the interaction between our synthesized ligands and the amino acid residues of the COX-1 protein (PDB code: 3N8Z), COX-2 protein (PDB code: 4m11) and of the penicillin binding protein 3 of Mycobacterium tuberculosis (6KGV). The docking finding demonstrates that ligand-protein binding happens in a manner consistent with executed constriction that interacts with the preferred manner. The float rating and docking score of recently

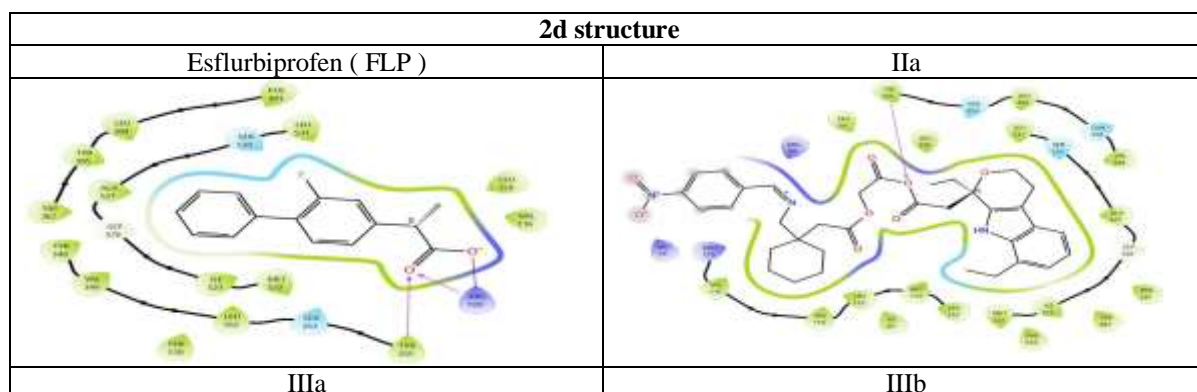
developed gabapentin -NSAIDs derivatives (IIa-IVb) were compared to usage of glide rating and docking score and potential strength activity. In docking study, the result shows that binding of ligand to protein occurs as consistent with carried out constriction with interplay with preferred way.

Anti-inflammatory study

The newly developed ligands and Esflurbi-profen (FLP) use as a reference were docked against three-dimen-sional structures of cyclogenes' enzyme COX1; and the Diclofenac use as a reference were docked against two-dimensional structures of cyclogeneses' enzyme COX 2 as shown in Table 2 and Figure 2.

Table 2. Anti-inflammatory docking scores of gabapentin-NSAIDs derivatives docked with receptors COX1 (PDB code 3N8Z) Esflurbiprofen (FLP) as reference ; and COX2 (PDB code: 4m11) Diclofenac as a reference .

COX-1			COX-2		
ID	ΔG (Kcal/mol)	Types of interaction	ID	ΔG (Kcal/mol)	Types of interaction
Esflurbiprofen (FLP)	-10.1	Salt bridge : with ARG120. H-bond : with TYR355 , ARG120.	Diclofenac	-6.228	Halogen bond:SER530 H-bond:ARG120 , TYR355. Pi-cation:ARG120
IIa	-4.84	H-bond : with Arg120	IIa	-6.594	H-bond : with ARG120. Pi- cation : ARG120, PHE518.
IIb	N.A	-	IIb	0.39	-
IIIa	-10.78	H-bond:Arg120 Pi-cation: with Arg83	IIIa	-7.249	H-bond with:Arg120 , TYR355. Pi-cation with: LYS83 , TYR386.
IIIb	-9.137	H-bond : with Arg120,TYR355,Arg120. Pi-Pi stacking : with TRP387, TYR385.	IIIb	-0.787	Halogen bond : with ARG513. H-bond : SER530.
IVa	-9.84	H-bond : with Arg120	IVa	-4.148	H-bond: with TYR385 , SER530 , PHE518.
IVb	-9.35	H-bond : with Arg120	IVb	-2.091	Halogen bond : with PHE518. H-bond : with SER530. Pi-cation :with ARG120.



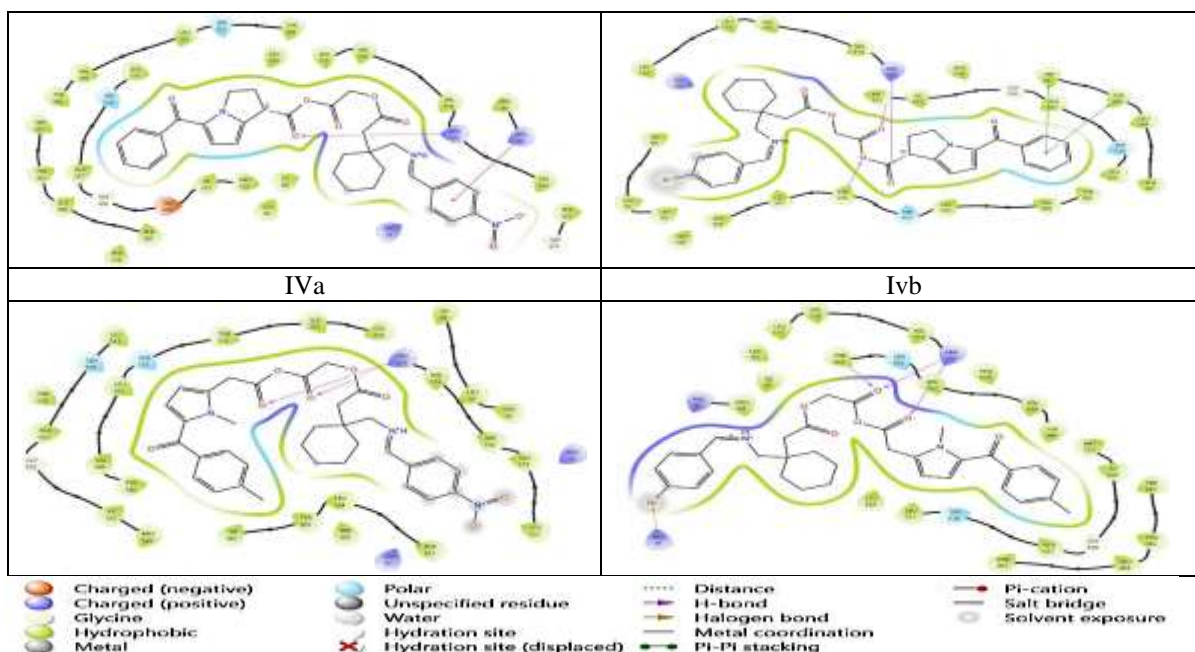


Figure 2. Anti-inflammatory docking/2d structure for compounds with cox1.

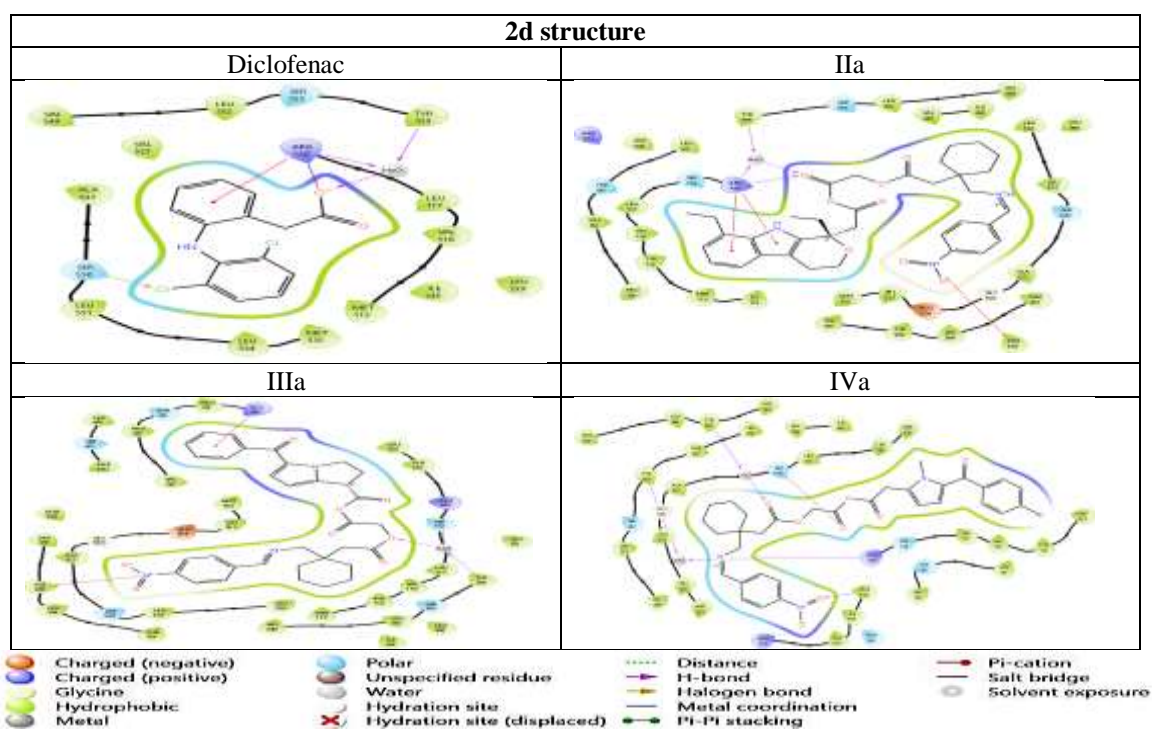


Figure 3. Anti-inflammatory docking/2d structure for compounds with cox γ .

The docking data (Table 2) demonstrate compound IIIa's potential affinity, as it scored -10.78 kcal/mol, somewhat better than that of the reference compound FLP, which scored -10.1. IIIa demonstrated a strong affinity by squeezing into the binding pocket and connecting with Arg120 to create an essential hydrogen bond. Furthermore, its nitrobenzene ring interacted pi-cationally with Arg83's protonated state, increasing the binding stability of the molecule. IIIa was unique because of its long conformation in the binding pocket, which allowed for wide interactions with other res-

idues. In contrast, the contact range of other ligands was limited due to their adoption of more folded conformations. Significantly, the inflexible triple fused ring ligands were unable to create a preferred extended structure within the binding site, probably as a result of their lack of flexibility.

Regarding FLP, it has showed a clear interaction with Arg120, highlighting the importance of this residue in the function of proteins. Remarkably, every ligand except for that from compound IIa and IIb was able to establish a minimum of one hydrogen bond with Arg120 inside the binding

region, indicating that Arg120 plays a crucial role in ligand-protein interactions. These results highlight the favorable binding affinity of compound IIIa and also underscore the importance of structural flexibility in enhancing ligand-protein interactions. Furthermore, finding important residues like Arg120 is very helpful for making smart designs for strong COX-1 inhibitors that work better as medicines. Unfortunately, **IIb** has failed to find suitable conformation for binding to the enzyme and as a result it has failed to give any score. The re-docking process confirmed the robustness of the initial docking results, emphasizing the favorable binding affinity of compound IIIa, and this can be considered as a validation process for the docking

technique as well. The docking data (Table 2) also demonstrate compound IIIa and IIa potential affinity with COX-2, as it scored -7.249 and -6.594 kcal/mol respectively, somewhat better than that of the reference compound Diclofenac, which scored -6.228. **IIIa** demonstrated a strong affinity by squeezing into the binding pocket and connecting with Arg120 and TYR355 to create an essential hydrogen bond

Antibacterial study

In antibacterial study, amoxicillin use as a reference and the synthesized compounds docked against penicillin binding protein 3 of *Mycobacterium tuberculosis* (PDB code 6KGV); as shown in table 3.

Table 3. Anti-bacterial docking scores: penicillin binding protein 3 of *Mycobacterium tuberculosis* (PDB code 6KGV), Amoxicillin as reference

ΔG (Kcal/ mol)	Docking score	Types of interaction
Amoxicillin (reference)	-3.8	H-bond : GLN597 , THR593 , THR595 , SER386 , ASN441.
IIa	-5	H-bond : THR593 , HIP422.
IIb	-5.81	H-bond : GLN597 , ASN443 , THR593.
IIIa	-8.22	H-bond : HIS645 , ASN443 , GLN597 , THR593. Pi-Pi stacking : with HIS645.
IIIb	-5.16	H-bond : ASN443 , SER441 , THR533 , GLN597.
IVa	-4.5	H-bond : GLN597 , THR593 , ASN443 , HIS645 , SER441.
IVb	-2	H-bond : SER441 , ASN443 , THR593 , HIS645 , GLN597

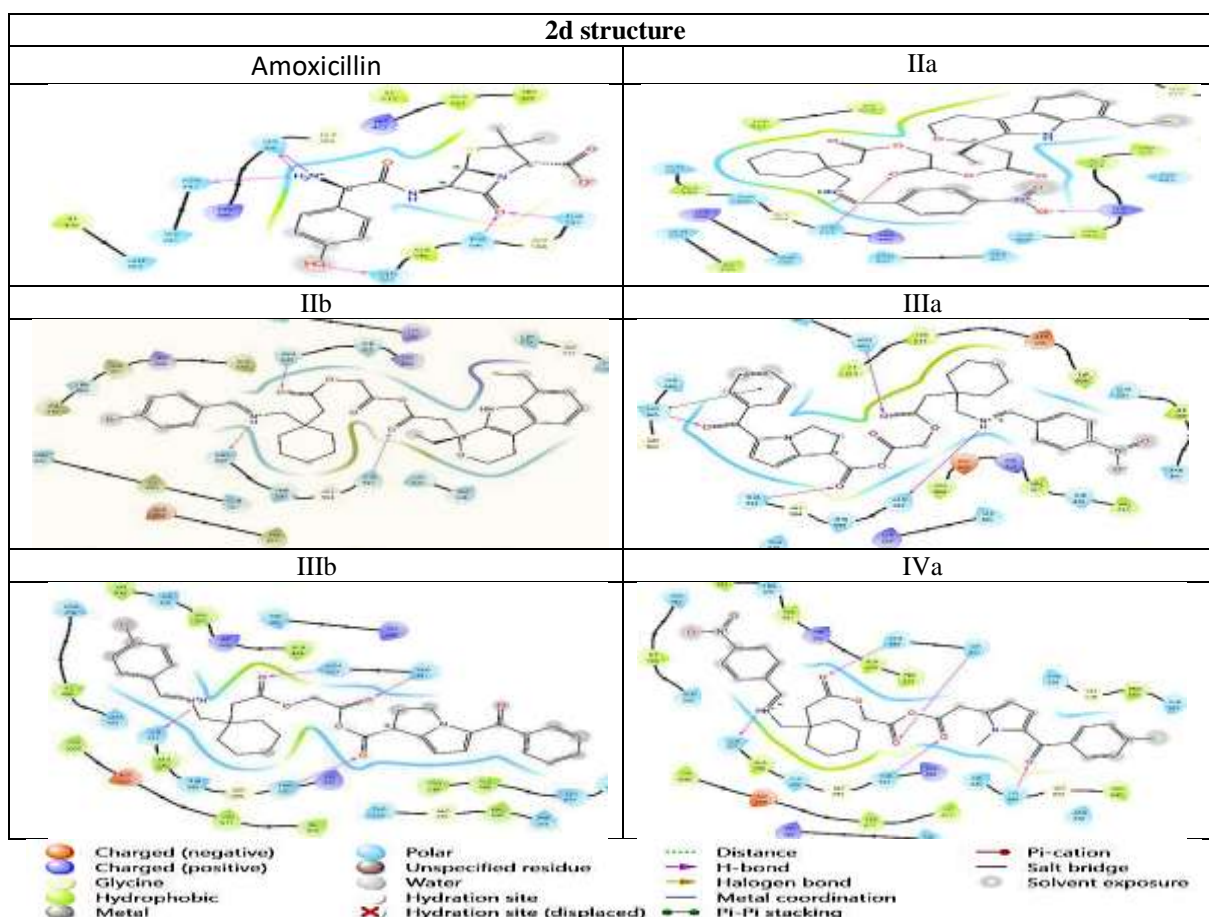


Figure 4. Anti-bacterial docking/2d structure for compounds.

By examining the first crystal structure of 6KGV (also known as PBP3 in the Protein Data Bank), it was possible to gain understanding of the interaction between the protein and its co-crystallized ligand, amoxicillin. Several significant interacting residues have been detected. The amino acid residues Thr595, Thr593, Gln597, and Asn443 establish hydrogen bonds with the ligand, thereby enhancing its stability within the binding pocket. **IIa** has scored -5 kcal/mol upon docking into the binding site of the PBP3 of mycobacterium. A hydrogen bond has been established between the nitro group and HIP422, and the anhydride group and THR593.

IIb has obtained a score of -5.81, demonstrating the presence of H-bonds involving imine-GLN597, ester-ASN443, and anhydride-THR593. **IIIa** has achieved a score of -8.22, indicating that it is a highly bound ligand. It formed four hydrogen bonds with specific amino acids (ketone-HIS645, anhydride-THR593, ester-ASN443, Imine-GLN597), and a π - π stacking interaction was also found between acetophenone and HIS645. **IIIb** achieved a score of -5.16 and identified four hydrogen bonds: Imine-GLN597, ester-ASN443, Anhydride-SER441, and anhydride-THR593. **IVa** has

achieved a score of -4.5 and formed a total of 5 hydrogen bonds. These hydrogen bonds include Imine-GLN597, ester-ASN443, Anhydride-SER441, anhydride-THR593, and Acetophenone-HIS645. **IVb** received the lowest score of -2 and formed three H-bonds (Anhydride-ASN443, Anhydride-SER441, Ester-THR595), one π - π stacking (bromobenzene-TRP425), and one halogen bond (Br-LYS440). The test ligands, except for **IVb**, competed with and had stronger affinities for PBP3 than amoxicillin, which was used as a standard. The poor score of **IVb** can be attributed to its inability to adopt a stable conformation within the binding pocket, resulting in a less stable and less robust binding complex with the protein. Refer to Figure 3 for further details. The data indicate that these ligands, especially **IIIa**, can function as powerful inhibitors of PBP3 and exhibit significantly higher binding efficiency compared to Amoxicillin.

ADMET study

The prediction of ADMET properties using *in silico* methods is a crucial step in the drug development process, significantly enhancing the efficiency and accuracy of identifying viable drug candidates; as shown below in table 4.

Table 4. *in silico* ADMET prediction results of the final compounds.

Cpds.	Mol.wt	Rotatable bond	Donor HB	Accept HB	TPSA Å ²	LogP values		Rule of Five	logS values		
						iLOGP	Silicos-IT		ESOL	Ali	Silicos-IT
IIa	631.72	15	1	9	152.87	4.73	6.62	2	-6.86	-9.1	-9.67
IIb	665.61	14	1	7	107.05	5.55	9.44	1	-7.69	-9.03	-11.1
IIIa	599.63	14	0	9	149.85	4.25	4.19	2	-5.93	-7.66	-7.73
IIIb	633.53	13	0	7	104.03	4.53	7.01	1	-6.76	-7.59	-9.16
IVa	601.65	15	0	9	149.85	4.23	4.97	2	-6.32	-8.4	-8.31
IVb	635.54	14	0	7	104.03	5.09	4.79	1	-7.16	-8.33	-9.74
Recommended values	150-500	no more than 9 rotatable bonds	0-6	2-20	20-130 Å ²	-2 -6.5		Max 4	Insoluble<-10 Poorly<-6 Moderately<-4 Soluble<-2 Very soluble <0		

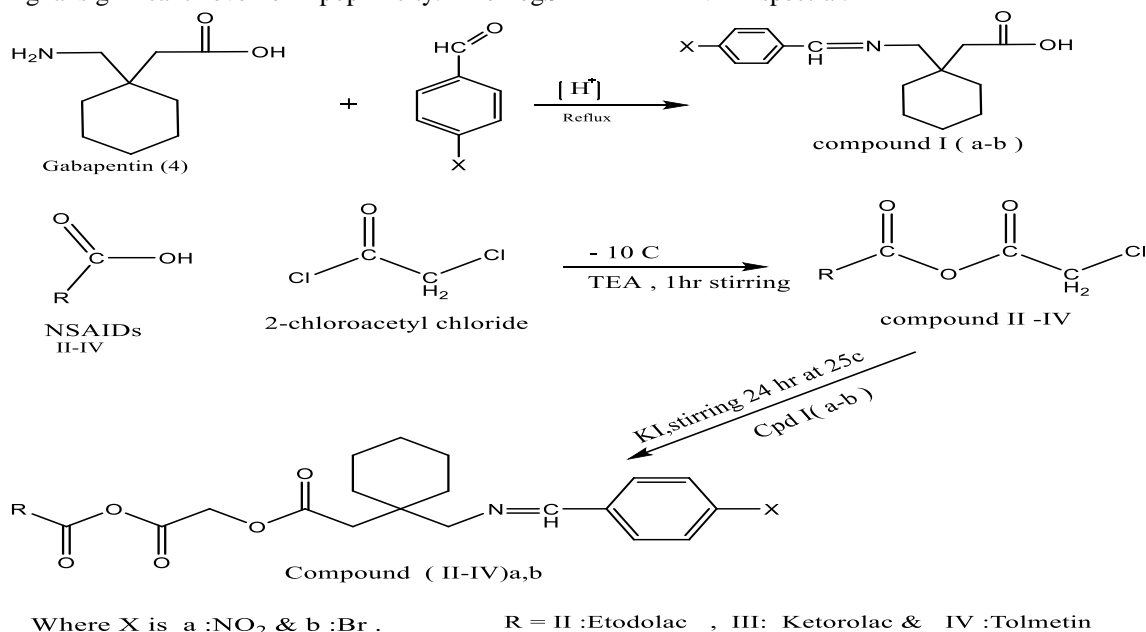
HBD: Estimated number of hydrogen bonds that would be donated by the solute to water molecules in an aqueous solution. **HBA:** Estimated number of hydrogen bonds that would be accepted by the solute from water molecules in an aqueous solution. **- logP iLOGP o/w:** Predicted logarithm octanol/water partition coefficient. **- Rule of Five:** Number of violations of Lipinski's rule of five. **- logS (Ali):** water solubility (calculated with the Ali model).

The compounds have a molecular weight ranging from 599.63 to 665.61 g/mol, suggesting the existence of relatively large molecules. The count of heavy atoms and aromatic heavy atoms ranges from 42 to 46, with a significant proportion being aromatic, namely 15 to 17. The value of the Csp3 percentage ranges from 0.36 to 0.49, suggesting a moderate degree of saturation. The number of rotatable bonds ranges from 13 to 15, indicating a good level of flexibility. The hydrogen bond acceptor count is within the range of 7 to 9, but the hydrogen bond donor count is either 0 or 1, suggesting a modest propensity for hydrogen bonding. The topological polar surface area (TPSA) exhibited significant values, ranging from 104.03 to 149.85, indicating a considerable extent of polar surface area. This has the potential to negatively impact the ability of substances to pass through and be absorbed by a material or organism. The LogP values for iLOGP, XLOGP3, WLOGP, MLOGP, and Silicos-IT are being referred to. The Log P values of these compounds range from 4.23 to 9.85, indicating a significant level of lipophilicity. The logS

values (ESOL, Ali, Silicos-IT) projected that the compounds will have low aqueous solubility, suggesting poor solubility. In the end, it is envisaged that these compounds will have minimal absorption in the gastrointestinal tract and will not be able to penetrate the blood-brain barrier. The bioavailability score usually varies from 0.17, whereas the synthetic accessibility score ranges from 4.40 to 5.43.

Synthetic studies

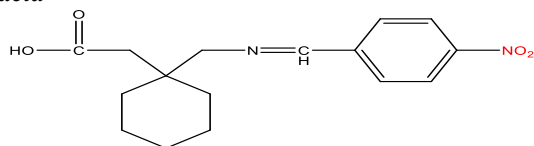
The overall process for synthesizing the intermediates and targeted compounds were depicted in Scheme 1 ; Gabapentin was reacted with two types of para-substituted benzaldehyde (*p*-Nitrobenzaldehyde, and *p*-bromobenzaldehyde) to protect the free amine group via converting it to imine (Schiff base) (1a-b) , Esterification by the reaction of NSAID with chloroacetyl chloride to give the corresponding ester II-IV , The reaction of II-IV with 1a-b(to give the final product (IIa-IVb). The characterization and functional groups of the proposed compounds were identified by using the IR spectroscopy, their structures were confirmed by ¹H-NMR spectra .



Scheme1. Synthesis of intermediates Ia-b and targeted compounds IIa-IVb

Synthesis of gabapentin- *p*-substituted benzaldehyde schiff base

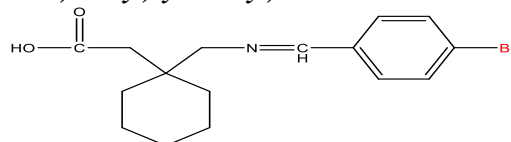
• **Compound (Ia) :** 2- (1- (((4-nitro benzylidene) amino) methyl) cyclohexyl) acetic acid



light brown powder. , yield=86%,m.p=(92-93) °C, (R_f =0.5,Chloroform:ethyl acetate:ether 10:5:1), IR(ν=cm⁻¹): broad band at 3329.5 – 3260.5 cm⁻¹ owing to OH group , 3064.32 (Stretching vibration

of CH (aromatic)) , 2846.93 and 2735.06 (C-H Str of CH₂), 1705.07 (C=O)str. of COOH, 1647.21 (C=N)str. of imine, 1604.77 (C=C)str, 1517 asym and 1381.03 sym. Str. Vib.NO₂) str. 3105(C-O) str. of COOH .

• **Compound (Ib) :** 2-(1-(((4-bromobenzylidene)amino)methyl)cyclohexyl)acetic acid



brown powder, yield=82%,m.p=(155-157) °C,(R_f =0.8, Chloroform:ethyl acetate:ether 10:5:1) ,

IR(ν = cm^{-1}): broad band at 336794.5 – 3247.5 cm^{-1} owing to two OH group 2816.07, and 2904.80 (C-H Str. of CH_2), 1658.78 (C=O) str. of COOH, 1589.34 (C=N) str. of imine, 1581.26 (C=C) str., 725.23 (C-Br) str.

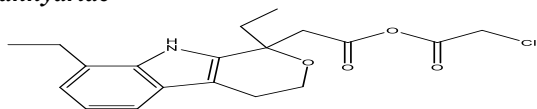
The reaction of the primary amine group in gabapentin is crucial to prevent side reactions during the synthesis of target compounds, the formation of imines from the reaction of primary amines with aldehydes or ketones is influenced by several factors, including electronic and steric effects. Schiff bases derived from aromatic substituted benzaldehydes have a wide range of applications, including in the fields of coordination chemistry, catalysis, and biological activities. Aromatic substituted benzaldehydes are generally more readily available and easier to handle compared to aliphatic aldehydes, making them a convenient choice for the synthesis of Schiff bases^(20,42). This stability is attributed to the resonance stabilization provided by the aromatic ring, making aromatic imines more suitable for various applications.⁽⁴³⁾

Glacial acetic acid plays a multifaceted role in the synthesis of Schiff bases, which is crucial for ensuring efficient and selective reactions. It helps maintain an acidic pH environment. This acidic environment is necessary for the formation of the imine (Schiff base) as it facilitates the nucleophilic attack of the amine on the carbonyl carbon of the aldehyde or ketone, making the carbonyl carbon more electrophilic and susceptible to nucleophilic attack. Additionally, the protons provided by glacial acetic acid act as a catalyst, promoting the dehydration step where water is eliminated to form the imine product. The use of glacial acetic acid also improves the selectivity of the Schiff base formation, suppressing side reactions and maximizing the yield of the desired product^(20,44).

The IR spectrum of the intermediates Ia, and Ib indicated to the disappearance of broad, strong absorption due to the N-H stretching vibration of the primary amine group ($-\text{NH}_2$) around 3300 cm^{-1} , and to the revealed bands that attributed C=N Stretching vibration of imine group str. at (Ia: (1647.21), and Ib: (1589.34)) cm^{-1} respectively.

Synthesis of NSAIDs -chloroacetyl chloride derivatives comps. (II - VI)

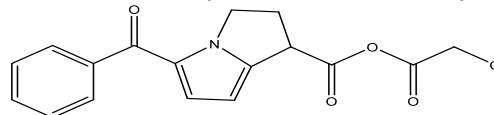
•Compound (II) 2-chloroacetic 2-(1,8-diethyl-1,3,4,9-tetrahydropyrano(3,4-b)indol-1-yl)acetic anhydride



Brown powder, yield=72%, m.p.=167-169 °C, ($R_f = 0.6$, Toluene : ethyl acetate 2:1), IR(ν = cm^{-1}): 3340 (asy N-H of pyrrole), 3055.24 Stretching vibration of CH (aromatic), 2970.38

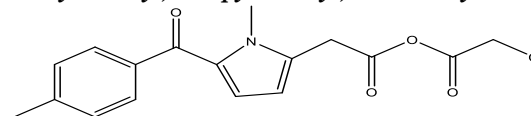
and 2931.80 Stretching vibration of CH_2, CH_3 (aliphatic), 1739.79 and 1705.07 (ester C=O) str., 1589.37 (C=C) str., 1458.18 C-N-C asymmetric stretch (aromatic), 1411.89 Aromatic C-C stretching vibrations, 1261.45 C-O-C asymmetric stretch for anhydride, 1033.85 C-O-C asymmetric stretch ether, 837.11 C-C-O symmetric stretch ether, 794.67 C-Cl Stretching vibration.

•Compound (III) 5-benzoyl-2,3-dihydro-1H-pyrrolizine-1-carboxylic 2-chloroacetic anhydride



Brown, yield=69%, m.p.=(150-152) °C, ($R_f = 0.8$, Toluene : ethyl acetate 2:1), IR(ν = cm^{-1}): 3055.24 Stretching vibration of CH (aromatic), 2924.09 and 2951.09 C-H stretching vibrations of CH_2, CH_3 (aliphatic groups), 1739.79 Saturated symmetric C=O stretch (strongest), 1670.35 Saturated asymmetric C=O stretch, 1593.20 C=C stretching vibrations of the aromatic ring, 1566.20 C-N-C asymmetric stretch (aromatic), 1473.62 aromatic C-C stretching vibrations, 1265.30 C-O-C asymmetric stretch for anhydride, 790.81 C-Cl Stretching vibration.

•Compound (IV) 2-chloroacetic 2-(1-methyl-5-(4-methylbenzoyl)-1H-pyrrol-2-yl)acetic anhydride



White powder, yield=76%, m.p.=(174-176) °C, ($R_f = 0.8$, Toluene : ethyl acetate 2:1), IR(ν = cm^{-1}): 3115.04 and 3028.24 Stretching vibration of CH (aromatic), 2958.80 C-H stretching vibrations of CH_2, CH_3 (aliphatic groups), 1730.15 Saturated symmetric C=O stretch (strongest), 1703.14 Saturated asymmetric C=O stretch, 1512.49 C=C stretching vibrations of the aromatic ring, 1568.13 C-N-C asymmetric stretch (aromatic), 1487.12 Aromatic C-C stretching vibrations, 1265.30 C-O-C asymmetric stretch for anhydride, 736.81 C-Cl Stretching vibration.

Chloroacetyl chloride is a highly reactive acylating agent, making it suitable for esterification reactions due to its increased electrophilicity, which facilitates nucleophilic attack by OH of alcohols. Chloroacetyl chloride can be used in the presence of other functional groups, such as halogens, without causing unwanted side reactions or affecting the esterification process⁽⁴⁵⁾. The synthesis of the intermediate as NSAIDs -chloroacetyl chloride (II-IV) were synthesized from three types of NSAIDs (a-Etodolac, b-Ketorolac, and c-Tolmetin) with chloroacetyl chloride. The conversion of chloroacetyl chloride into ester, will occur through nucleophilic acyl substitution reactions which involve tetrahedral intermediate Nucleophilic substitution at the acyl carbon atom in α -

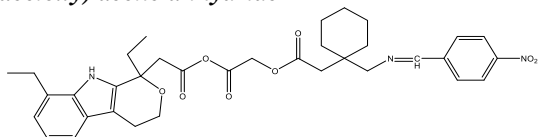
chloroacetyl chloride is highly selective due to the pronounced electrophilicity of the carbonyl carbon, which is significantly influenced by the presence of two electron-withdrawing groups: the doubly bonded oxygen and the chlorine atom. This heightened electrophilicity makes the carbonyl carbon more susceptible to nucleophilic attack compared to the alkyl one in alkyl chlorides⁽⁴⁶⁾.

The reaction is carried out with trimethylamine (TEA) which is useful in acylation reactions, particularly for neutralizing hydrogen chloride, is well-documented and advantageous due to its nucleophilicity and ability to act as an electron-releasing group (ERG). TEA's nucleophilicity is higher compared to NSAIDs, making it a preferred choice in such reactions⁽⁴⁷⁾. The necessity of maintaining low temperatures by, such as below -10°C , is crucial because it helps control the reaction kinetics and prevents the decomposition of reactive intermediates, optimizing esterification reactions, ensuring high yields, and maintaining the stability of the reactants and catalysts involved⁽⁴⁸⁾.

The IR spectrum of the intermediates II, III and IV indicated to the disappearance of broad bands of NSAIDs hydroxyl group (-OH) and to the revealed bands that attributed ester(C=O) str. at (II: (1739.79, 1705.07), III: (1739.79, 1670.35), and IV: (1730.15, 1703.14) cm^{-1} respectively.

Synthesis of Target Compounds (IIa-IVb)

• **Compound (IIa)** 2-(1,8-diethyl-1,3,4,9-tetrahydropyrano(3,4-b)indol-1-yl)acetic 2-(2-(1-(4-nitrobenzylidene)-amino) methyl) cyclohexyl) acetoxy) acetic anhydride

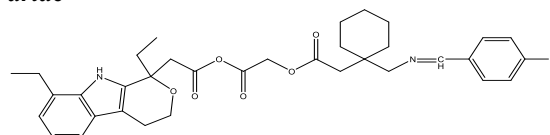


Yellow powder, yield=86%, m.p.=(180-182) $^{\circ}\text{C}$, ($R_f = 0.5$, Chloroform : methanol 85:15) IR($\nu=\text{cm}^{-1}$): 3340.71 (N-H of pyrrole) asymmetric stretching vibrations, 3093.82 Stretching vibration of CH (aromatic), 2924.09 C-H stretching vibrations of CH_2 (aliphatic groups), 1793.80 Saturated symmetric C=O stretch (strongest), 1732.08 Saturated asymmetric C=O stretch, 1678.07 C=N Stretching vibration of imine group, 1593.20 & 1570.06 C=C stretching vibrations of the aromatic ring, 1477.47 C-N-C asymmetric stretch (aromatic), 1400.32 Asymmetric N-O stretching vibration of the nitro group, 1342.46 Symmetric N-O stretching vibration of the nitro group, 1265.30 C-O-C asymmetric stretch for anhydride, 1083.99 C-O-C asymmetric stretch ether.

¹H NMR(500 MHz, DMSO-d₆; δ ,ppm): 1.16-1.42 (m,6H methyl groups), 1.85-1.90(m, 6H, cyclohexane ring of gabapentin), 1.94-(m,4H cyclohexane ring of gabapentin), 2.15 (CH₂ of ethyl group of pyran), 2.27 (s,2H, α CH₂ to cy-

clohexane ring of gabapentin), 2.41 (t, 2H, CH₂ of pyran ring), 3.00 (s, 2H, α -CH₂ to pyran ring), 3.03 (t,2H,CH₂ of ethylbenzene), 3.05 (s, 2H, α CH₂ to C=N), 3.77 (t, 2H, CH₂ of pyran ring), 5.42 (s,2H, α CH₂ to two ester groups), 6.79 (d, 2H, benzene ring), 7.14-7.18 (m, 1H, benzene ring), 7.64 (d, 2H, m-nitrobenzene ring), 7.86 (d, 2H,o- nitrobenzene ring), 8.20 (s,1H, Schiff base proton) and 10.94 (s, 1H, NH pyrrole).

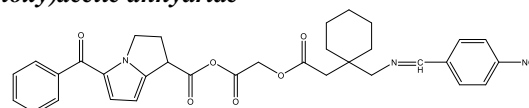
• **Compound (IIb):** 2-(2-(1-(((4-bromobenzylidene) amino)methyl) cyclohexyl)acetoxy) acetic 2-(1,8-diethyl-1,3,4,9-tetrahydropyrano(3,4-b)indol-1-yl)acetic anhydride



Brown powder, yield=81%,m.p.=(211-213) $^{\circ}\text{C}$, ($R_f = 0.7$, Chloroform : methanol 85:15), IR($\nu=\text{cm}^{-1}$): 3305.99 (N-H of pyrrole) asymmetric stretching vibrations, 3020.53 Stretching vibration of CH (aromatic), 2920.23 and 2854.65 C-H stretching vibrations of CH_2 (aliphatic groups), 1691.06 Saturated symmetric C=O stretch (strongest), 1651.07 Saturated asymmetric C=O stretch, 1630.09 C=N Stretching vibration of imine group, 1580.49 & 1512.19 C=C stretching vibrations of the aromatic ring, 1485.19 C-N-C asymmetric stretch (aromatic), 1280.73 C-O-C asymmetric stretch for anhydride, 1072.42 C-O-C asymmetric stretch ether, 844.82 C-O-C symmetric stretch ether, 675.09 C-Br.

¹H NMR (500 MHz, DMSO-d₆; δ ,ppm): 1.12-1.32 (m,6H methyl groups), 1.74-1.79(m, 6H, cyclohexane ring of gabapentin), 1.81-1.84 (m,4H cyclohexane ring of gabapentin), 2.27 (t, 2H, CH₂ of ethyl group of pyran), 2.35 (s,2H, α CH₂ to cyclohexane ring of gabapentin), 2.57 (t, 2H, CH₂ of pyran ring), 2.78(s, 2H, α -CH₂ to pyran ring), 2.83 (t, 2H, CH₂ of ethylbenzene), 3.05 (s, 2H, α CH₂ to C=N), 3.48 (t, 2H, CH₂ of pyran ring), 4.92 (s,2H, α CH₂ to two ester groups), 6.73 (d, 2H, benzene ring), 6.76-6.82 (m, 1H, benzene ring), 7.57 (d, 2H, o-bromo-benzene ring), 7.68 (d, 2H,m- bromobenzene ring), 8.68 (s,1H, Schiff base proton) and 9.68 (s, 1H, NH pyrrole).

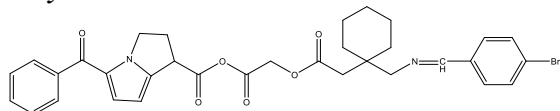
• **Compound (IIIa):** 5-benzoyl-2,3-dihydro-1H-pyrrolizine-1-carboxylic 2-(2-(1-(((4-nitrobenzylidene) amino)-methyl)cyclohexyl) acetoxy)acetic anhydride



Pale yellow powder, yield=81%, m.p = (234.5-236)°C, (R_f = 0.8, Chloroform : methanol 85:15), IR(ν =cm⁻¹): 3105.39 and 3082.25 Stretching vibration of CH (aromatic), 2850.79 C-H stretching vibrations of CH₂ (aliphatic groups), 1778.37 Saturated symmetric C=O stretch (strongest), 1705.07 Saturated asymmetric C=O stretch, 1604.77 C=N Stretching vibration of imine group, 1582.67 & 1527.62 C=C stretching vibrations of the aromatic ring, 1446.61 C-N-C asymmetric stretch (aromatic), Aromatic C-C stretching vibrations, 1342.46 the asymmetric and symmetric stretching of the nitro (NO₂) group, 1284.59 C-O-C asymmetric stretch for anhydride.

¹HNMR (500 MHz, DMSO-d₆; δ , ppm): 1.21-1.27 (m, 6H, cyclohexane ring of gabapentin), 1.58-1.68 (m, 4H cyclohexane ring of gabapentin), 1.87 (dt, 2H, CH₂ of pyrrolizine ring), 3.58 (s, 2H, α CH₂ to cyclohexane ring of gabapentin), 3.63 (s, 2H, α CH₂ to C=N), 3.80 (t, 1H, CH of pyrrolizine ring), 3.87 (t, 2H, CH₂ of pyrrolizine ring), 4.80 (s, 2H, α CH₂ to two ester groups), 7.09 (d, 1H, pyrrolizine ring), 7.46 (d, 1H, pyrrolizine ring, β of α,β -unsaturated system), 7.90-7.92 (m, 7H, benzene ring), 7.86 (d, 2H, benzene ring), 8.05 (d, 2H, m-nitrobenzene ring), 8.27 (d, 2H, o-nitrobenzene ring), 8.48 (s, 1H, Schiff base proton).

• **Compound (IIIb): 25-benzoyl-2,3-dihydro-1H-pyrrolizine-1-carboxylic 2-(2-(1-(((4-bromobenzylidene) amino) methyl) cyclohexyl)acetoxy)acetic anhydride**

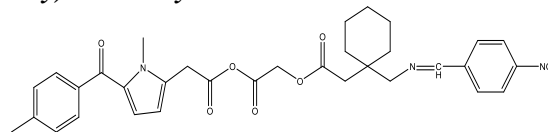


Brown powder, yield=79%, m.p=(187-188)°C, (R_f = 0.7, Chloroform : methanol 85:15), IR(ν =cm⁻¹): 3086.11 and 3039.81 Stretching vibration of CH (aromatic), 2924.09 and 2885.51 C-H stretching vibrations of CH₂ (aliphatic groups), 1724.34 Saturated symmetric C=O stretch (strongest), 1701.22 Saturated symmetric C=O stretch, 1631.78 C=N Stretching vibration of imine group, 1570.06 & 1512.49 C=C stretching vibrations of the aromatic, 1465.90 C-N-C asymmetric stretch (aromatic), 1257.59 C-O-C asymmetric stretch for anhydride, 586.36 C-Br stretching.

¹HNMR (500 MHz, DMSO-d₆; δ , ppm): 1.25-1.27 (m, 6H, cyclohexane ring of gabapentin), 1.31-1.33 (m, 4H cyclohexane ring of gabapentin), 1.36 (dt, 2H, CH₂ of pyrrolizine ring), 1.58 (s, 2H, α CH₂ to cyclohexane ring of gabapentin), 1.60 (s, 2H, α CH₂ to C=N), 2.22 (t, 1H, CH of pyrrolizine ring), 4.14 (t, 2H, CH₂ of pyrrolizine ring), 5.32 (s, 2H, α CH₂ to two ester groups), 7.43 (d, 1H, pyrrolizine ring), 7.77 (d, 1H, pyrrolizine ring, β of α,β -unsaturated system), 7.81-7.85 (m, 7H, benzene ring), 8.17 (d, 2H, benzene ring), 8.22

(d, 2H, m-bromobenzene ring), 8.29 (d, 2H, o-bromobenzene ring), 8.53 (s, 1H, Schiff base proton).

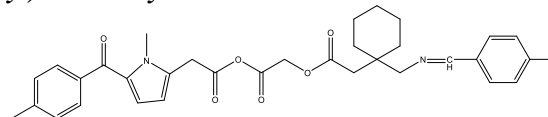
• **Compound (IVa): 2-(1-methyl-5-(4-methyl benzoyl)-1H-pyrrol-2-yl)acetic 2-(2-(1-(((4 nitrobenzylidene) amino) methyl) cyclohexyl) acetoxy)acetic anhydride**



Yellow-pale orange powder, yield=84%, m.p=(233-235)°C, (R_f =0.8, Chloroform : ethyl acetate : ether 62.5 : 31.25 : 6.25) IR(ν =cm⁻¹): 3078.39 and 3005.10 Stretching vibration of CH (aromatic), 2962.66, 2808.38 and 2885.51 C-H stretching vibrations of CH₂ (aliphatic groups), 1774.51 Saturated symmetric C=O stretch, 1670.35 Saturated asymmetric C=O stretch, 1585.49 C=N Stretching vibration of imine group, 1591.23 & 1561.48 C=C stretching vibrations of the aromatic ring, 1496.76 C-N-C asymmetric stretch (aromatic), 1531.48 & 1400.32 the asymmetric and symmetric stretching of the nitro (NO₂) group, 1269.16 C-O-C asymmetric stretch for anhydride.

¹HNMR (500 MHz, DMSO-d₆; δ , ppm): 1.10-1.19 (m, 6H, cyclohexane ring of gabapentin), 1.20-1.23 (m, 4H cyclohexane ring of gabapentin), 2.33 (s, 2H, α CH₂ to cyclohexane ring of gabapentin), 3.05 (s, 3H, toluene ring), 3.47 (s, 2H, α CH₂ to C=N), 3.60 (s, 2H, α CH₂ to C=O), 3.88 (s, 3H, N-CH₃), 4.89 (s, 2H, α CH₂ to ester), 7.26 (d, 1H, pyrrole ring), 7.55 (d, 1H, pyrrole ring, β of α,β -unsaturated system), 7.61 (d, 2H, benzene ring), 7.81 (d, 2H, benzene ring), 7.94 (d, 2H, o-bromobenzene ring), 8.05 (d, 2H, m-bromobenzene ring), 8.42 (s, 1H, Schiff base).

• **Compound (IVb): 2-(2-(1-(((4-bromo benzylidene) amino) methyl) cyclohexyl)acetoxy)acetic 2-(1-methyl-5-(4-methylbenzoyl)-1H-pyrrol-2-yl)acetic anhydride**



Brown, yield=77%, m.p=(198-199.5)°C, (R_f =0.6, Chloroform : ethyl acetate : ether 62.5 : 31.25 : 6.25), IR(ν =cm⁻¹): 3020.31 Stretching vibration of CH (aromatic), 2908.65 and 2858.51 C-H stretching vibrations of CH₂ (aliphatic groups), 1735.93 Saturated symmetric C=O stretch, 1685.83 Saturated asymmetric C=O stretch, 1631.78 C=N Stretching vibration of imine group, 1570.06 & 1527.62 C=C aromatic stretching vibrations, 1485.19 C-N-C asymmetric

stretch, 1269.16 C-O-C asymmetric stretch for anhydride, 605.65 C-Br stretching.

¹H-NMR (500 MHz, DMSO-d₆; δ, ppm) : 1.30-1.39(m, 6H, cyclohexane ring of gabapentin), 1.95-2.35 (m, 4H cyclohexane ring of gabapentin), 2.63 (s, 2H, α-CH₂ to cyclohexane ring of gabapentin), 2.92 (s, 3H, toluene ring), 3.35 (s, 2H, α-CH₂ to C=N), 3.69 (s, 2H, α-CH₂ to C=O), 3.83 (s, 3H, N-CH₃), 5.93 (s, 2H, α-CH₂ to ester), 7.24 (d, 1H, pyrrole ring), 7.29 (d, 1H, pyrrole ring, β of α,β-unsaturated system), 7.43 (d, 2H, benzene ring), 7.48 (d, 2H, o-bromobenzene ring), 7.54 (d, 2H, m-bromobenzene ring), 7.58 (d, 2H, benzene ring), 8.45 (s, 1H, Schiff base).

The IR spectrum of final derivatives (IIa - IVb) indicated the disappearance of broad band of OH group of: Etodolac (3255.84-3209.55) cm⁻¹, ketorolac (3371.57-3216.58) cm⁻¹, tolmetin (3226.73-3255.24) cm⁻¹ and the appearance of band attributed ester(C=O)str for (II-IV)a,b respectively: {(1732.08, 1793.80), (1732.08, 1793.80), (1778.37, 1705.07), (1724.34, 1701.22), (1774.51, 1670.35) and (1716.65, 1631.78) cm⁻¹} on the other hand, the interpretation of the ¹H-NMR spectrum for compounds IIa-Vb revealed a singlet peak due to the (CH₂ α to ester group) and there is no peak appeared at the range of proton of carboxylic group.

In the synthesis of the target compounds, which are mutual prodrugs of gabapentin, were synthesized with the aid of different types of NSAIDs such as (Etodolac, Ketorolac and Tolmetin) and para substituted benzaldehyde in addition to chloroacetyl spacer (-OCH₂COO-). The conversion of chlorinated esters to iodinated esters using triethylamine (TEA) and sodium iodide in dimethylformamide (DMF), then mix the iodinated ester with gabapentin in the presence of TEA\DMF. Replacement of chloride with iodide by reacting the chlorinated ester (resulted from step 2) with anhydrous NaI because removal of

iodide in the next step is easier than that of chloride. (Finkelstein reaction, halo-de-halogenation)⁽⁴⁹⁾. Sodium iodide is employed due to its ability to facilitate nucleophilic substitution reactions, where the iodide ion (I⁻) replaces the chlorine atom in the ester. Additionally, the presence of iodide ions can significantly accelerate the reaction rate, triethylamine (TEA) serves as a base in this reaction, neutralizing any acidic by-products and maintaining an optimal pH for the reaction to proceed efficiently. TEA also helps in deprotonating intermediates, thereby facilitating the nucleophilic attack by iodide ions. The choice of DMF as the solvent is further justified by its ability to stabilize reaction intermediates and its high boiling point, which allows the reaction to be conducted at elevated temperatures, thereby increasing the reaction rate and yield⁽⁵⁰⁾.

¹H-NMR Spectrophotometer

The interpretation of the ¹H-NMR spectrum for compounds IIa-Vd revealed a singlet peak due to the (CH₂ α to ester group) at δ= (ppm): IIa 4.93, IIb 4.98, IIIa 5.01, IIIb 4.98, IVa 5.11, IVb 5.17, respectively and there is no peak appeared at the range of proton of carboxylic group. All the inferences mentioned above provide evidence of the occurrence of the association and the success of the preparation of the compounds.

Preliminary Pharmacological Studies

Anti-Inflammatory Activity^(43, 51)

The subcutaneous injection of egg-white into the rat paw produces inflammation resulting from plasma extravasations, increased water tissue and plasma protein exudation along with neutrophil extravasations, which are all due to the metabolism of arachidonic acid. Comparison of the Diclofenac Sodium (Standard) effect on the control (Propylene Glycol) The results were summarized with in Figure (4) and Table (5)

Table 5. Effect of Diclofenac Sodium (Standard) and Propylene Glycol(control) on egg white induced paw edema in rats.

Period of time (hours)	Thickness of Paw (mm)	
	Control	Standard
0	4.49 ±0.03	4.44 ±0.02
1/2	4.72 ±0.02	4.58 ±0.02
1	6.06 ±0.03	6.00 ±0.04
2	7.67 ± 0.5	6.35 ±0.02***
3	7.76 ±0.03	6.11 ±0.01***
4	6.98 ±0.02	5.83 ±0.01***
5	6.57 ±0.11	5.25 ±0.02***

Data are expressed as mean ± SEM of mm paw thickness= 6 (number of animals). Significantly different compared to control: p-value *** ≤ 0.0001

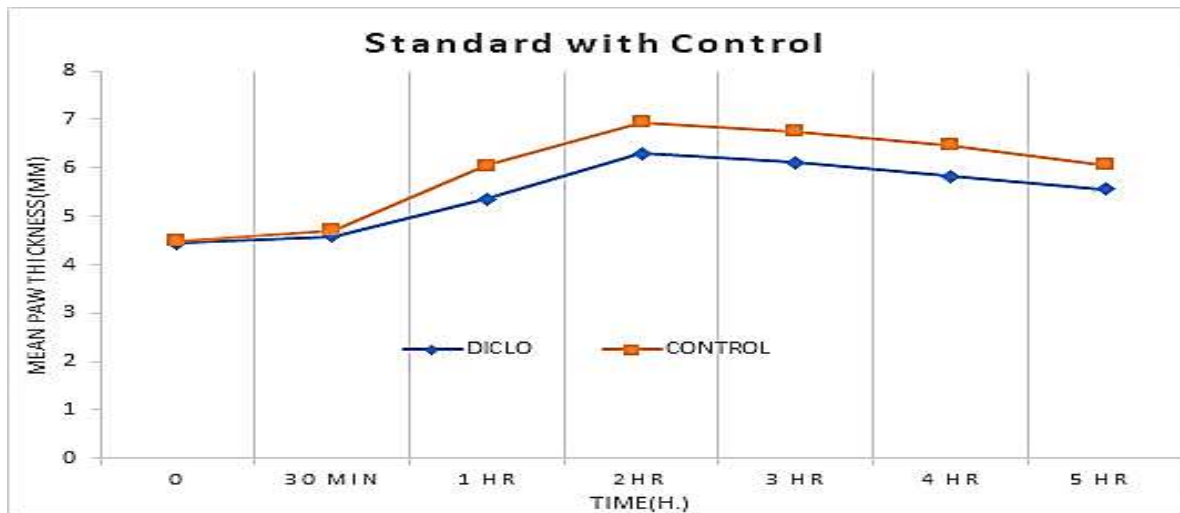


Figure 5. Effect of Diclofenac Sodium (Standard), Propylene glycol (control) on egg white induced paw edema in rats

Anti-inflammatory Effect of Tested Compound

Table (6) shows the effect of tested compounds on egg-white induced edema as an indicator for their anti-inflammatory activity. The intra-

plantar injection of egg-white into rat hind paw induce a progressive edema, which was reached maximum (measured by millimeter) after 1 hour of injection.

Table 6. Anti-inflammatory activity of control, slandered and gabapentin derivatives on egg white induced paw edema in rat

	Time(h.)	0 h.	0.5 h.	1h.	2 h.	3 h.	4 h.	5 h.
Paw Thickness (mm)	Control	4.49 ±0.03	4.72 ±0.02	6.00 ±0.03	7.67± 0.5	7.76 ±0.03	6.97 ±0.02	6.56 ±0.11
	standard	4.44 ±0.02	4.58 ±0.02	6.00 ±0.04	6.35 ±0.02***	6.11 ±0.01***	5.83 ±0.01***	5.24 ±0.02***
	II a	4.43 ±0.02	4.67 ±0.02	6.006 ±0.04	6.15 ±0.01*	5.17 ±0.03***	5.08 ±0.02***	4.85 ±0.04***
	II b	4.61 ±0.01	4.68 ±0.01	5.97 ±0.01	6.66 ±0.04*	6.42 ± 0.4*	6.41 ±0.01***	6.32 ±0.01**
	III a	4.52 ±0.02	4.66 ±0.02	5.95 ±0.03	6.52 ±0.01*	6.06 ±0.01*	5.11 ±0.02***	4.75 ±0.01***
	IIIb	4.55 ±0.03	4.67 ±0.02	6.00 ±0.03	7.00 ±0.02***	6.88 ±0.01***	6.68 ±0.02***	6.54 ±0.02**
	IVa	4.47 ±0.01	4.64 ±0.02	5.99 ±0.02	6.73 ±0.01***	6.47 ±0.03***	6.18 ±0.02***	5.96 ±0.04***
	IV b	4.50 ±0.01	4.64 ±0.02	5.94 ±0.05	6.46 ±0.01*	6.15 ±0.01*	6.07 ±0.02***	5.31 ±0.01*

Different testing groups' non-identical superscripts (a, b) are evaluated as significantly different ($p \leq 0.05$). Data are expressed as mean \pm SEM of mm paw thickness, n= number of animal, time (0) is time of injection of tested compounds time (30) min is time of injection of egg-white (induced by paw edema), *significantly different with control ($p \leq 0.05$) All tested compounds and standard drug showed significant activity in comparison with control at 2 hrs. time. * (IIa, IVa, IIb & IVb) compounds showed activity comparable to standard drugs and significantly higher than control from time (2-5)hrs. * (IIIa & IIIb) compounds showed lower activity than standard; Control from time (2-5)hrs.

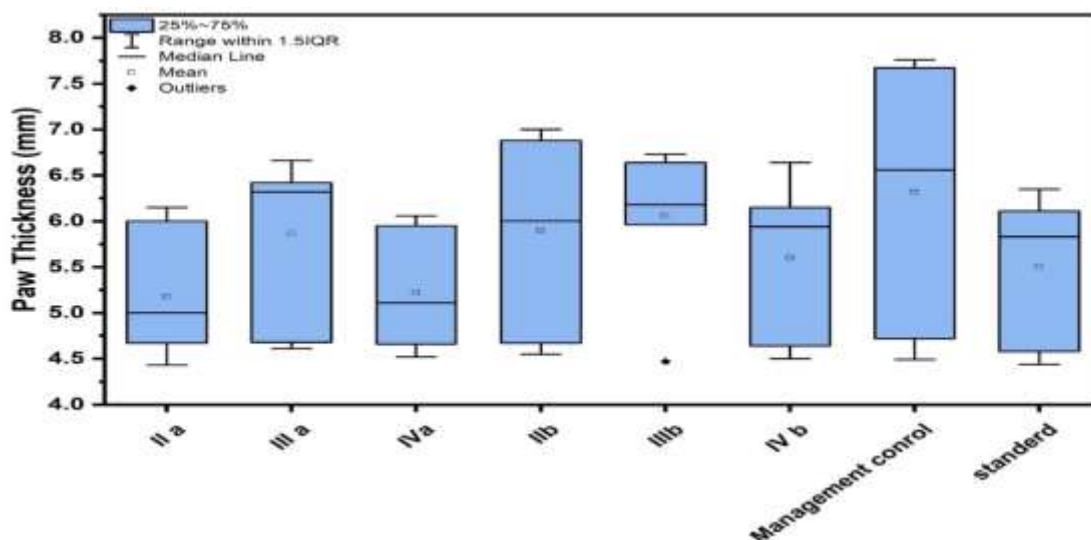


Figure 6. Curves illustrates anti-inflammatory activities of final compounds in comparison with control and standard.

Compounds (IIa-IVb) exhibitioner in comparison with diclofenac effect also to derivatives (IIa-IVb) produced signi-ficant reduction of paw edema with respect to the effect of propylene glycol; the anti-inflammatory assessment of the tested compound in comparison experimental chemicals with the control (propylene glycol 50%), they all displayed thinner paws thickness⁽²⁴⁾.

As shown in figure (5) and Table (6), there is no significant difference between the control and the final synthesized compounds (IIa-IVb) at time 0 and 1/2 h., 1h. while at 2h. these final compounds showed high significant difference when compared with the control, the strong significant difference of these in reduction of paw edema are compounds (IIa, IVa), while the rested compounds (IIIa, IIb) no significant difference in reduction of paw edema After 2-5 h. the other compounds (IIIb, IVb) showed significant effect in reduce paw edema.

- Compound IIa demonstrated significant anti-inflammatory activity over the time period from 0 to 5 hours, with a mean±SD of 5.18±0.65 and a p-value of less than 0.05. Similarly,
- Compound IIIa showed significant effects with a mean±SD of 5.86±0.85 and a p-value of less than 0.00001.
- Compound IIb, the mean±SD was 5.90±1.0 with a p-value of less than 0.0004.
- Compound IIIb had a mean±SD of 6.06±0.76 with a p-value of less than 0.0007.

The management control group showed significant results with a mean±SD of 6.32±1.3 and a p-value

of less than 0.0001. The standard treatment group also demonstrated significant effects with a mean±SD of 5.50±0.76 and a p-value of less than 0.0001. The t-test further indicated significant differences between the compounds and experimental chemicals at various time points. At the initial time point (0 hours).

- significant differences were observed among Compounds IIa, IIIa, IVa, IIb, IIIb, IVb, the management control, and the standard, with a p-value of 0.0001.
- At 30 minutes, significant differences persisted among these groups, with a p-value of 0.00002. At 1 hour, the p-value was 0.00006, at 2 hours it was 0.00001,
- at 3 hours it was 0.00005, at 4 hours it was 0.00005, and at 5 hours it remained significant with a p-value of 0.00005.

These findings indicate that all tested compounds exhibited significant anti-inflammatory effects over the studied period in comparison to the experimental chemicals and control, with each compound showing distinct levels of efficacy at different time point.

Antibacterial Activity

The synthesized final compounds (IIa-IVd) were tested to evaluate their anti-microbial activity towards gram -, gram + also anti-fungi (fluconazole is standard compounds), by well penetrated diffusion type method .While the antibacterial solubilizer was amoxicillin and ciprofloxacin. DMSO was the solvent and as control.

Table 7. MIC values for gabapentin derivatives (IIa-IVd); ciprofloxacin , amoxicillin and fluconazole as standard.

compounds	MIC (mm)						
	Gram positive bacteria			Gram negative bacteria			Fungi
	<i>S. aureus</i>	<i>S. pneumonia</i>	<i>B. subtilis</i>	<i>E. coli</i>	<i>P. aeruginosa</i>	<i>K. pneumoniae</i>	<i>Candida albicans</i>
	Conc.(mcg/ml)						
Amoxicillin	125	250	125	125	250	250	
Ciprofloxacin	125	125	125	125	125	125	
Fluconazole	-	-	-	-	-	-	125
DMSO	<i>as a solvent and control</i>		<i>as a solvent and control</i>		<i>as a solvent and control</i>		
IIa	500	1000	500	500	500	1000	500
IIb	500	500	500	500	1000	1000	500
IIIa	500	500	500	500	1000	1000	1000
IIIb	500	500	500	500	1000	1000	500
IVa	1000	1000	1000	1000	-	-	1000
IVb	250	250	250	250	500	500	250

Table 8. Antimicrobial activity as of final compounds(IIa-IVd) as Inhibition zone .

Zone of inhibition mm	<i>S. aureus</i>	<i>S. pneumonia</i>	<i>B. Subtilis</i>	<i>E. coli</i>	<i>P. aeruginosa</i>	<i>K. pneumoniae</i>	<i>C. albicans</i>	Control G-	DMSO
IIa	32	29	28	30	20	30	27	-	-
IIb	27	25	23	25	17	29	27	-	-
IIIa	29	28	25	26	20	20	23	-	-
IIIb	30	28	26	27	27	33	26	-	-
IVa	26	25	23	25	21	27	24	-	-
IVb	37	33	36	35	34	36	31	-	-
Amoxicillin	40	38	38	39	37	37		-	-
Ciprofloxacin	39	35	37	33	32	32		-	-
Fluconazole							36	-	
Mean ±SD	32.5 ±5.4	30.1 ±4.73	29.5 ±6.43	30 ±5.20	26 ±7.55	30.5 ±5.42	27.7 ±4.46	--	--
SEM	1.93	1.67	2.27	1.84	2.67	1.91	1.68	--	--
P (value)	0.000*	0.00000*	0.000*	0.000*	0.000*	0.000*	0.000*	--	--

NS: No Significant Value * (P<0.05)

The inhibition zones of the chemical being tested are considered to be extremely active when they are more than 15 mm, moderately active when they are between 10 and 15 mm, barely active when they are between 5 and 10 mm, and inactive when they are less than 5 mm. The synthesized final compounds (IIa–IVb) were tested to evaluate their antimicrobial activity against gram negative, gram positive bacteria and fungi, this evaluation was done using well diffusion method, using the standard compounds with antifungal agent was (fluconazole), while with antibacterial agent was

(Amoxicillin and ciprofloxacin); DMSO was chosen as a solvent and as control⁽⁵²⁾.

As observed from Table (8), the mean ± SD for *S. aureus* is 32.5 ± 5.4. The T-test indicates a strong correlation between the Zone of Inhibition (IIa–IVb, Amoxicillin, Ciprofloxacin, Fluconazole) and *S. aureus*, with a p-value less than 0.05. Similarly, for *S. pneumonia*, the mean ± SD is 30.1 ± 4.73, and the T-test shows a strong correlation with the same set of inhibitors, with a p-value less than 0.000.

• *B. subtilis* has a mean \pm SD of 29.5 ± 6.43 , and the T-test indicates a strong correlation with the Zone of Inhibition (IIa, IIb, IIIa, IIIb, IVa, Amoxicillin, Ciprofloxacin, Fluconazole), with a p-value less than 0.0000. For *E. coli*, the mean \pm SD is 30 ± 5.20 , and the T-test also shows a strong correlation with the same inhibitors, with a p-value less than 0.000.

• *P. aeruginosa* exhibits a mean \pm SD of 26 ± 7.55 , and the T-test reveals a strong correlation with the Zone of Inhibition (IIa, IIb, IIIa, IIIb, IVa, Amoxicillin, Ciprofloxacin, Fluconazole), with a p-value less than 0.0001. *K. pneumoniae* has a mean \pm SD of 30.5 ± 5.42 , with the T-test showing a strong correlation with the inhibitors, resulting in a p-value less than 0.000.

• *C. albicans*, with a mean \pm SD of 27.7 ± 4.46 , also shows a strong correlation with the Zone of Inhibition (IIa, IIb, IIIa, IIIb, IVa, Amoxicillin, Ciprofloxacin, Fluconazole), with a p-value less than 0.000. The data demonstrate that all tested microorganisms exhibit a strong correlation between the Zone of Inhibition and the set of inhibitors (IIa, IIb, IIIa, IIIb, IVa, Amoxicillin, Ciprofloxacin, and Fluconazole).

• *S. aureus* and *S. pneumoniae*: Both pathogens show significant susceptibility to the inhibitors, as indicated by their respective mean values and low p-values. The mean \pm SD for *S. aureus* (32.5 ± 5.4) and *S. pneumoniae* (30.1 ± 4.73) suggest that the inhibitors are highly effective against these bacteria, with relatively consistent results. In summary, the inhibitors tested are broadly effective against a range of bacterial and fungal pathogens.

The consistently low p-values across different microorganisms highlight the robustness of these inhibitors. However, the variability in the Zone of Inhibition, particularly for *P. aeruginosa*, indicates that while the inhibitors are generally effective, their efficiency can vary significantly between different strains or conditions. Further studies might explore the reasons behind these variations and optimize the inhibitors for even broader and more consistent application.

Conclusion

The synthesis of a new series of gabapentin-NSAIDs derivatives was accomplished with successful results. There is somewhat a noticeable relationship between the docking results of our compound and the results of the *in vitro* results. Also they showed accepted pharmacokinetic properties through the virtual ADMET studies. Although these compounds demonstrate favorable bioavailability scores, their elevated lipophilicity, inadequate solubility, and likelihood of metabolic interactions pose obstacles that require attention during further stages of therapeutic development.

The MIC results show that compound (IVb) can inhibit a variety of bacterial strains at low concentrations when compared to another synthetic

compounds. According to the MIC and zone of inhibition results, compound (IVb) is more active against the fungi (*C. albicans*) than another compounds.

Recommendations for further studies

• A preliminary hydrolysis research was conducted on the synthesized target compounds in diluted plasma and at two different pH levels (1.2 and 7.4) to demonstrate the potential for chemical or enzymatic hydrolysis of these potential mutual products.

• Study the toxicity activity of the synthesized derivatives; also study the anticancer activity as cell lines to reveal on which-on-which type of cancer cells also have activity.

Acknowledgment

The authors are grateful to the College of Pharmacy/ University of Baghdad; for all the facilities to conduct the research, also our thanks and appreciations to Assist..

Conflicts of Interest

The authors declare that they have no known competing financial interests or personal relationships that could have appeared to influence the work reported in this paper.

Funding

The authors declare that they have no received financial support from an Institution.

Ethics Statements

The authors declare that their study does not need ethical approval from an ethics committee.

Author Contribution

Both authors contributed to the research study design and practical application of the research strategy for the preparation of target compounds for which FTIR and ¹HNMR tests were conducted on, and interpretation of their results. As well as conducting antimicrobial and anti-inflammatory tests and discussing their results; also, both authors reviewed the complete research writing in terms of scientific and linguistic formulation.

References

1. Konovalova, I.S., et al., Crystal structure of the non-steroidal anti-inflammatory drug (NSAID) tolmetin sodium. Acta Crystallographica Section E: Crystallographic Communications, 2021. **77**(2): p. 134-137.
2. Sohail, R. Effects of non-steroidal anti-inflammatory drugs (NSAIDs) and gastroprotective NSAIDs on the gastrointestinal tract: a narrative review. Cureus, 2023. **15**(4).p 21-29.
3. Shah, K. and G. Krishna, Chemical Characterization and Pharmacological

- Evaluation of Phytophenols-Etodolac Mutual Prodrugs. *Iraqi Journal of Pharmaceutical Sciences* (P-ISSN 1683-3597 E-ISSN 2521-3512), 2023. **32**(3): p. 49-59.
4. Kolawole, O. and K. Kashfi, NSAIDs and cancer resolution: new paradigms beyond cyclooxygenase. *International journal of molecular sciences*, 2022. **23**(3): p. 1432.
 5. Asthana, A., S. Tripathi, and R. Agarwal, A systematic review and meta-analysis of randomized control trials to check role of non-steroidal anti-inflammatory drugs as protective factor in Alzheimer disease subjects. *Advances in Alzheimer's Disease*, 2023. **12**(1): p. 1-16.
 6. Thiruchenthooran, V., E. Sánchez-López, and A. Gliszczynska, Perspectives of the application of non-steroidal anti-inflammatory drugs in cancer therapy: Attempts to overcome their unfavorable side effects. *Cancers*, 2023. **15**(2): p. 475.
 7. Nafie M. NSAID-Induced Lower Gastrointestinal Bleeding: A Case Report. *World Journal of Colorectal Surgery*, 2024. **13**(2): p. 49-53.
 8. McCarberg, B.H. and B. Cryer, Evolving therapeutic strategies to improve nonsteroidal anti-inflammatory drug safety. *American journal of therapeutics*, 2015. **22**(6): p. e167-e178.
 9. Kumari, R. and S. Agarwal, Role of Proton Pump Inhibitors in the Management of Peptic Ulcer. *International Journal of Pharmaceutical Sciences and Nanotechnology*, 2023. **16**(6): p. 7070-7080.
 10. Ortiz, M.I., Synergistic interaction and activation of the opioid receptor-NO-CGMP-K⁺ channel pathway on peripheral antinociception induced by the α -Bisabolol-diclofenac combination. *Frontiers in Pharmacology*, 2023. **14**: p. 1158236.
 11. Sehajpal, S., Prasad N., and Singh K., Prodrugs of non-steroidal anti-inflammatory drugs (NSAIDs): a long march towards synthesis of safer NSAIDs. *Mini reviews in medicinal chemistry*, 2018. **18**(14): p. 1199-1219.
 12. Akter M., Synthesis of Naproxen Esters and Evaluation of their In vivo and In silico Analgesic and Anti-inflammatory Activities. *Dhaka University Journal of Pharmaceutical Sciences*, 2023. **22**(1): p. 105-114.
 13. Holenarsipur V.K, Absorption and cleavage of enalapril, a carboxyl ester prodrug, in the rat intestine: in vitro, in situ intestinal perfusion and portal vein cannulation models. *Biopharmaceutics & drug disposition*, 2015. **36**(6): p. 385-397.
 14. De Souza, H.M., et al., Comparative chemical and biological hydrolytic stability of homologous esters and isosteres. *Journal of Enzyme Inhibition and Medicinal Chemistry*, 2022. **37**(1): p. 718-727.
 15. Shaaya O. Anhydride prodrugs for nonsteroidal anti-inflammatory drugs. *Pharmaceutical research*, 2003. **20**: p. 205-211.
 16. Perez, H.L., D. Knecht, and M. Busz, Overcoming challenges associated with the bioanalysis of an ester prodrug and its active acid metabolite. *Bioanalysis*, 2017. **9**(20): p. 1589-1601.
 17. Ngo, K.T., Evaluating Poly (anhydride-ester) Encapsulation Characteristics for Delivery of Hydrophobic Small Molecules. 2022.
 18. Frimayanti N., Nasution M., and Syah F. In silico approach through molecular docking and study ADME on imine derivative compounds as a potential antibacterial agent against *Staphylococcus aureus*. *Pharmacy Education*, 2024. **24**(2): p. 9-16.
 19. Feng, X. Green synthesis and antibacterial/fungal studies of two new Schiff base derived from 4-(imidazol-1-yl) benzaldehyde. *Indian Journal of Chemistry (IJC)*, 2022. **61**(3): p. 298-304.
 20. Omar TN. Synthesis of anti-inflammatory aromatic Schiff bases Synthesis of Schiff Bases of Benz-aldehyde and Salicylaldehyde as Anti-inflammatory Agents. *Iraqi JPharmSci*. 2007;16(2):5–11.
 21. Banasiak A. Gabapentin as a drug with a broad potential. Presentation of its use in medical conditions beyond the official registration. *Journal of Education, Health and Sport*, 2022. **12**(11): p. 127-132.
 22. Nudelman, A., Mutual Prodrugs-Codrugs. *Current Medicinal Chemistry*, 2023. **30**(38): p. 4283-4339.
 23. Yang Y . Efficient exploration of chemical space with docking and deep learning. *Journal of Chemical Theory and Computation*, 2021. **17**(11): p. 7106-7119.
 24. Lu, C. OPLS4: Improving force field accuracy on challenging regimes of chemical space. *Journal of chemical theory and computation*, 2021. **17**(7): p. 4291-4300.
 25. Daina, A., O. Michielin, and V. Zoete, SwissADME: a free web tool to evaluate pharmacokinetics, drug-likeness and medicinal chemistry friendliness of small molecules. *Sci Rep* 7: 42717. 2017.
 26. Nawaz, H., et al., Synthesis and biological evaluations of some Schiff-base esters of ferrocenyl aniline and simple aniline. *Journal of Organometallic Chemistry*, 2009. **694**(14): p. 2198-2203.
 27. Mallesha, L., Mohana K., and Veeresh B., Synthesis and biological activities of Schiff bases of gabapentin with different aldehydes and ketones: a structure-activity relationship

- study. Medicinal Chemistry Research, 2012. **21**: p. 1-9.
28. Furniss, B.S., Vogel's textbook of practical organic chemistry. 2011: Pearson Education India.
 29. Manon, B. and Sharma D., Design, synthesis and evaluation of diclofenac-antioxidant mutual prodrugs as safer NSAIDs. 2009.
 30. Mohammed, Z.B. and T.N. Omar, Chemical design, Synthesis and biological evaluation of mutual prodrug of Gabapentin with different types of phenolic and alcoholic antioxidants. Sys Rev Pharm, 2021. **12**(1): p. 858-868.
 31. Saha P.,Brishty S., and Rahman S., Pharmacological screening of substituted benzimidazole deriva-tives. Dhaka University Journal of Pharmaceutical Sciences, 2021. **20**(1): p. 95-102.
 32. Kanaan, S. and T.N. Omar, Synthesis and Preliminary Anti-Inflammatory and Anti-Microbial Evaluation of New 4, 5-Dihydro-1H-Pyrazole Derivatives. Iraqi Journal of Pharmaceutical Sciences (P-ISSN 1683-3597 E-ISSN 2521-3512), 2023. **32**(Suppl.): p. 262-270.
 33. Raauf AMR, Omar TNA, Mahdi MF, Fadhil HR. Synthesis, molecular docking and anti-inflammatory evaluation of new trisubstituted pyrazoline derivatives bearing benzenesulfonamide moiety. Nat Prod Res. 2022;1-21.
 34. Al-Nakeeb MR, Omar TNA. Synthesis, characterization and preliminary study of the anti-inflammatory activity of new pyrazoline containing ibuprofen derivatives. Iraqi J Pharm Sci. 2019;28(1):133-9.
 35. Elshikh M. Resazurin-based 96-well plate microdilution method for the determination of inhibitory concentration of biosurfactants. Biotechnology letters, 2016. **38**: p. 1015-1019
 36. Kavanagh A. Effects of microplate type and broth additives on microdilution MIC susceptibility assays. Antimicrobial agents and chemotherapy, 2019. **63**(1): p. 10.1128/aac.01760-18.
 37. Pradeep, P. and Suneetha V., Minimum Inhibitory Concentration (MIC) Of various synthetic and natural antimicrobial agents using E coli screened from VIT sewage treatment plant. International Journal of Chem. Tech Research, 2015. **8**(11): p. 287-291.
 38. Biswas T. Schiff Bases: Versatile Mediators of Medicinal and Multifunctional Advancements. Letters in Organic Chemistry, 2024. **21**(6): p. 505-519.
 39. Jordan A. Replacement of less-preferred dipolar aprotic and ethereal solvents in synthetic organic chemistry with more sustainable alternatives. Chemical reviews, 2022. **122**(6): p. 6749-6794.
 40. Omar TNA, Mahdi MF, Al-Mudhafar MMJ, Zainabbassim. Synthesize of new ibuprofen and naproxen sulphonamide conjugate with anti-inflammatory study and molecular docking study. Int J Pharm Qual Assur. 2018;9(2):102-8..
 41. Sun C.Highly Efficient Synthesis of Chlorogenic Acid Oleyl Alcohol Ester under Non-Catalytic and Solvent-Free Conditions. Molecules, 2023. **28**(9): p. 3948.
 42. Gallegos, M., A. Costales, and A. Martin Pendas, A real space picture of the role of steric effects in SN2 reactions. Journal of computational chemistry, 2022. **43**(11): p. 785-795.
 43. Tian J. Chemoselective N-Acylation of Amines with Acylsilanes under Aqueous Acidic Conditions. Organic Letters, 2023. **25**(31): p. 5740-5744.
 44. J's, H., Nucleophilic substitution at the carbonyl group. Organic chemistry, 2012: p. 196.
 45. Gao Y. Effects of a triethylamine catalyst on curing time and electro-optical properties of PDLC films. RSC Advances, 2013. **3**(45): p. 23533-23538.
 46. Soćko, R. and M. Kupczewska-Dobecka, Is dichloromethane an occupational carcinogen? Medycyna Pracy, 2007. **58**(2): p. 143-153.
 47. Morita, T., Y. Okamoto, and H. Sakurai, Novel method for dealkylation of esters, ethers, and acetals by chlorotrimethylsilane–sodium iodide. Journal of the Chemical Society, Chemical Communications, 1978(20): p. 874-875.
 48. Yeh,M. The Effect of Iodide Ion in Phase-Transfer Catalytic Syntheses of Benzyl Esters. Journal of the Chinese Chemical Society, 1991. **38**(3): p. 221-230.
 49. Ram R. and I. Charles, Unexpected Aromatization of 2-Acetoxy-3, 3-dichloro-4-(α -chloroalkyl) tetra-hydrofurans to 3-Alkyl-4-chlorofurans with NaI/DMF. Synthetic Communications®, 2008. **38**(12): p. 1946-1951.
 50. Heravi M., M. Ghavidel, and L. Mohammad, Beyond a solvent: triple roles of dimethylformamide in organic chemistry. RSC advances, 2018. **8**(49): p. 27832-27862.
 51. Edwards R, A reversible non-disruptive phase transition shown by the zinc iodide dimethylformamide complex ZnI₂ (dmf) 2. Acta Crystallographica Section B: Structural Science, 1998. **54**(5): p. 663-670.
 52. Magiorakos A. Multidrug-resistant, extensively drug-resistant and pandrug-resistant bacteria: an international expert proposal for interim standard definitions for acquired resistance. Clinical microbiology and infection, 2012. **18**(3): p. 268-281.

دراسة التصميم والتوليف والتقييم الدوائي الأولي لمضادات الالتهاب غير الستيروئيدية المترافقة مع الكابابنتين

نور وهاب صالح¹ و تغريد نظام الدين عمر^{2*}

¹ وزارة الصحة ، النجف الاشرف، العراق.

² قسم الكيمياء الصيدلانية، كلية الصيدلة، جامعة بغداد، بغداد، العراق.

الخلاصة

العقاقير المضادة للالتهابات غير الستيروئيدية تستخدم مضادات الالتهاب غير الستيروئيدية لعلاج مجموعة واسعة من حالات الألم ، وهي معروفة بخصائصها كمسكن وخافض للحرارة ومضاد للالتهابات.

التركيز على تصنيع مشتقات مضادات الالتهاب غير الستيروئيدية الجديدة (IIa-IVd) من خلال إدخال مجموعة الإستر في مجموعة COOH مع الجابابنتين من خلال رابط الأستيل.

تضمنت العملية تكوين قاعدة شيف؛ المركبات الوسيطات (Ia-b) من الجابابنتين والبارا بنزالدهيد . (اتودولاك، كيتورولاك، تولميتين) تخضع للأسترة بواسطة كلوريد الكلورو أسيتيل لتعطي الاسترات المقابلة (II-IV)، وأخيراً تفاعل Ia-d مع (II-IV) لينتج المشتقات النهائية (IIa-IVd) والتي تم التأكد من كفاءتها ودرجة النقاوة والتركيب بواسطة نقطة الانصهار (ATR-FTIR) و¹H-NMR. تم تقييم الأنشطة المضادة للالتهابات والمضادة للبكتيريا في المختبر وADME في محاكاة الحاسوب باستخدام Ligand Designer من Glide (مساحة عمل Schrödinger-2023-Maestro). بسبب تفاعل الرابطة الهيدروجينية مع الأحماض الأمينية الرئيسية في إنزيم COX1 مع المركبات (IIIa, IIIc, IIId) وتفاعل إنزيم COX-2 بالمركبات (IIIa, IIa) لديهم أعلى درجة الالتحام . فيما يتعلق بالنشاط المضاد للبكتيريا، فكلها مهمة باستثناء IVb فقط. حصلت

المركبات (IIIa, IIa & IIIc) على أعلى درجات الالتحام (-8.22، -7.07، -6.15) على التوالي. أظهر تحليل ADME أعلى النتائج مثل (IIa) -; (IIIa, IVa & IIc): (TPSA, IIb, IIC, IId) كمنح لرابطة الهيدروجين؛ - كمستقبل للرابطة الهيدروجينية (IIa, IIIa, IIVa, IIc)؛ (IIb, IId & IIC)؛ -logS: (IIb, IId & IIC)؛ و (logP o/w: (IId, IIb & IIC)؛ وأخيرا الرابطة القابلة للتدوير: (IIc, IVa & IVc)؛ تقع نتائج فحص insilico ADMET للمركبات الأخرى ضمن التوصيات الموصى بها الكلمات المفتاحية: الحركة الدوائية ، المضادة للبكتيريا ،كابابنتين ،الرسو الجزيئي، مشتقات مضادات الالتهابات الالاستروئيدية، الايتودولاك، الكيتورولاك ،التولميتين .